N63-22167

ER-4809

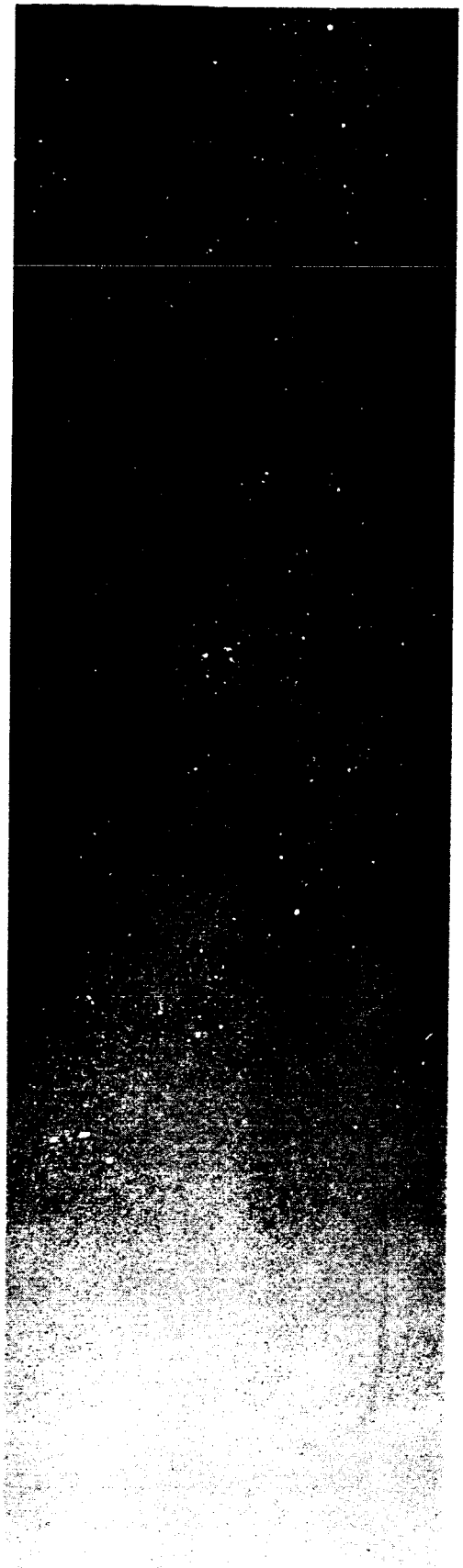

MEASUREMENT OF THERMAL PROPERTIES OF LiH AND LiH-Li MIXTURES: ENTHALPY, HEAT OF FUSION, CONDUCTIVITY

TOPICAL REPORT

THE WORK PRESENTED IN THIS REPORT WAS FUNDED BY NASA UNDER CONTRACT NAS 5-462.

JUNE 1962

TRW

TAPCO a division of
Thompson Ramo Wooldridge Inc.

14

PROJECT

512-238131-08

MEASUREMENT OF THERMAL PROPERTIES OF
LiH AND LiH-Li MIXTURES
ENTHALPY, HEAT OF FUSION, CONDUCTIVITY

ER 4809

PREPARED BY:	CHECKED BY:	APPROVED BY:
J. W. Vogt		James J. Owens
J. W. Vogt Research Chemist		James J. Owens, Manager Advanced Materials Development

DATE

October 15, 1961

DEPARTMENT

Advanced Materials Development

Thompson Ramo Wooldridge Inc.

CLEVELAND, OHIO, U. S. A.

TABLE OF CONTENTS

FIGURES

TABLES

ABSTRACT

22167

Measurements were made over the temperature range of 600-800°C, of the enthalpies of LiH and of LiH-Li mixtures in the molar proportions 90:10, 80:20, and 70:30. From the data are derived the specific heat of solid and molten material and the heat of fusion.

Thermal conductivity was measured for molten LiH and solid LiH at the melting point.

SUMMARY

Values obtained for the heat of fusion and specific heat of "pure" LiH and LiH-Li mixtures are the following:

Molar Ratio	ΔH_f	Specific Heat Below M.P.	Specific Heat Above M.P.
100 LiH-0 Li	659 cal g^{-1}	2.087 cal $g^{-1}deg\ C^{-1}$	1.762 cal $g^{-1}deg\ C^{-1}$
88.9 LiH-11.1 Li	600	1.977	1.792
80.1 LiH-19.9 Li	528	2.352	1.542
69.9 LiH-30.1 Li	461	2.173	1.681

Thermal conductivity of molten LiH, through the temperature range 710° to 770°C, declined from 0.0112 to 0.0094 cgs. units. These values are subject to considerable question inasmuch as they are roughly three times greater than the values previously reported for solid LiH.

1.0 Introduction

This project was undertaken to provide data concerning lithium hydride properties for the Sunflower program. Lithium hydride, as a thermal energy storage material, is maintained at, or near the melting point, with melting and freezing processes providing the major heat sink capacity. The LiH is expected to lose hydrogen during prolonged service in space and therefore the material is transformed from LiH to an LiH-Li mixture.

Many of the pertinent thermal properties of LiH and LiH-Li mixtures have not been measured heretofore. The specific heat, enthalpy, and heat of fusion have been reported for commercially pure LiH only. Thermal conductivity has been reported only for solid LiH, and at temperatures only well below the melting point. (Ref. 1, 2, 3, 4).

Therefore this project was intended to measure the specific heats, enthalpies, heats of fusion, and thermal conductivities of LiH and LiH-Li mixtures, (100 to 70 mol % LiH) in the solid and liquid states.

The calorimetric measurements for specific heat, enthalpy, and heats of fusion were completed for specimens of varying Li content. Thermal conductivity measurements were completed on pure LiH, but were not attempted with LiH-Li mixtures. In addition to time, and other limitations, there was the basic problem of maintaining a constant LiH-Li proportion in spite of hydrogen loss by diffusion. Moreover, according to the phase diagram for the Li-LiH system (Figure 19) the material in the composition range of interest exists in two phases. The measurement of thermal conductivity of LiH-Li mixtures thus proved to be of an entirely different complexity than was originally recognized. And, in addition, it seemed that the measured conductivity of a stratified Li-LiH system is unrelated to the dispersed type of mixture that is most likely to develop in a system in space. However, some data are presented for what may be the Li-rich phase in a two-phase system, and the calculated conductivity is in a plausable order.

2.0 Dry Box

One phase of the project was the acquisition and equipping of a dry box. Drawing from the experiences of several consultants, the decision favored a vacuum-purge type box, the advantages of which are that vacuum purging is positive and measurable, that the problems and inconveniences of circulating purification systems are avoided, and that system leaks to the atmosphere are detectable as vacuum leaks.

Attainment of 0.1 micron pressure is accepted as evidence of adequate purging; the box is back-filled with gettered argon gas, and operations in the inert atmosphere are completed quickly. The box is immediately evacuated again and maintained under vacuum during all idle periods.

After a general inquiry to all known builders of such equipment the Model A-12 box (S. Blickman Co., New Jersey) was procurred. It was fabricated from polished stainless steel, included a vacuum purge entrance lock, and included several modifications, such as provision for connection to a 4-inch vacuum system (2-inch connection to the lock), entry for electric welding equipment and vacuum line, and a floor opening for possible attachment of a cylindrical furnace. The vacuum system included a Welch Duoseal Pump (Model 1397), a 4-inch oil diffusion pump, a 4-inch copper line to the box, and a 2-inch branch line to the lock. Pressure was measured to 0.01 micron by a Stokes McLeod gage. The pressure in box and lock could easily be reduced to 0.03 microns and the leak rate did not exceed 7 microns per hour.

3.0 Enthalpy Measurement

3.1 General Considerations

Measurements of enthalpy and heat of fusion were made with two drop-type adiabatic calorimeters constructed as part of the project. Although the inherent superiority of the Bunsen ice calorimeter in many kinds of measurements is recognized, it seemed unlikely that that type of apparatus could be built, perfected, and adapted to the particular problem within the time allotted. The adiabatic aneroid type is capable of adequate precision, and, with the use of automatic control and recording equipment, seemed more appropriate for the project. To a considerable degree, the selection was influenced by the experience of H. E. Hoffman's group at ORNL. They had attempted to use the ice calorimeter in work of this kind and had reluctantly abandoned it as a method impractical within their framework for the type of measurement desired. Their subsequent experience with the copper block calorimeters had been entirely satisfactory in general and specifically in measurements on pure LiH. Our calorimeters were therefore built as copies of those at ORNL.

The calorimeters and the entire thermel system were standardized against synthetic sapphire, for which thermal data have been reported by the National Bureau of Standards. The sapphire was contained in a metal capsule like those used to contain the LiH specimens, and the procedure was like that used with the specimens. Thermal capacity (or the calorimeter constant) was expressed in Joules per millivolt change of thermopile potential.

Both specific heat and heat of fusion are derived from measurements of enthalpy change of the specimen in cooling from an original temperature near the melting point to some given final temperature at which it is in equilibrium with the calorimeter. Selection of the common final temperature is purely arbitrary and is based on convenience. One may adjust the initial conditions to produce a final calorimeter temperature reasonably near the selected temperature and then apply a correction based on the known thermal capacities, or alternatively, one may select the initial temperature conditions carefully to ensure a final temperature very close to the selected value. The latter course was adopted. The final calorimeter temperature selected was 30°C and the initial calorimeter temperature was carefully adjusted on each occasion to the value which would lead to the final value of 30°C. Usually, the error in an acceptable measurement was less than 0.2°C.

Enthalpy changes were measured for each specimen for initial specimen temperatures ranging from 600 to 800°C. A plot of these enthalpy changes against initial specimen temperature includes an abrupt rise at the melting point, the contribution of heat of fusion to the total enthalpy change.

3.2 Description of Apparatus

3.2.1 Calorimeter Construction

Each calorimeter consists of a copper block within a water-tight metal shell, which is in turn submerged in a water bath. The copper block (Figure 1) is 4 1/2 inches in diameter and 6 inches high and has a tapered specimen receiving well that extends nearly to the bottom. A gate is provided at the top to admit the specimen and close off the cavity after entry. The longitudinal and peripheral grooves are mounting channels for the thermel leads (Figure 2). Each thermel bead was insulated with masking lacquer and bedded in paraffin in a thermel well, several of which are visible in Figure 2.

The copper block rested on low conductivity nylon posts at the bottom of the inner chamber and was separated from the metal surfaces by an air gap about one-inch thick. When assembled as shown in Figures 4 and 5, the copper block was sealed within the inner chamber, which rested on short metal posts within the outer water jacket.

Only the thermel leads and gate-operating handle extended through the inner chamber cover. Four electric water heaters were installed through holes provided in the bottom of the water chamber and a centrifugal water circulation pump was connected to the influent and effluent manifolds. When the water jacket was filled to the overflow level, the inner chamber cover was two inches below the surface and only the access tubes extended upward through the water. The inner chamber was thus almost completely enveloped in a water mantle the temperature of which was subject to control.

3.2.2 Thermel System

The thermel system (iron-constantan couples) consisted of three thermopiles--two mounted in the copper block and one in the water jacket. With the associated equipment, they performed three functions--measured the copper block temperature, maintained an adiabatic condition between the block and the surrounding water mantle, and made a continuous record of the block temperatures.

Twenty thermels in the copper block were connected to form one pile of eight units and another of twelve units. A second pile of eight units was located in the water mantle. All cold junctions were located in ice baths, and copper wire leads were extended to the switching system and measuring and control equipment. For each calorimeter the switching system provided two alternate thermel circuits:

Automatic Operation: The two 8 unit piles in the block and water jacket were connected as a differential pile to a Wheelco Capacitrol, which controlled the water heaters. (By connecting the thermel leads directly to the Capacitrol meter leads the maximum sensitivity of the instrument was used.) Thus, the heaters were controlled to maintain the water jacket temperature very close to that of the copper block.

The 12-unit pile in the block was connected to a multipoint recorder as a convenience to provide a visible continuous record of temperature changes of the block during preliminary adjustments and during the approach to final thermal equilibrium.

Measure: To achieve maximum sensitivity (about 0.001°C) in measuring the block temperature, the 8-unit and 12-unit piles in the block were connected in series to an L & N Type K-3 potentiometer for manual measurement. During this time, input signal to the Wheelco Capacitrol was interrupted, and undesired heating of the water jacket during the measuring interval would have occurred. A correction was effected by providing as an interim signal, the output of a thermel immersed in the ice bath and connected in reverse to deflect the meter upscale. The practice was adopted then of measuring the block temperatures during intervals when the water heaters were normally not operating; the normal off-on cycle of the heaters was thus undisturbed.

The water jacket control system was intended to maintain temperature equality with the copper block at all times, but it did not succeed completely. During several minutes of rapid temperature rise of the block following specimen drop, the four 1000 watt heaters were unable to prevent a considerable thermal lag in the water jacket. This deficiency was corrected by injecting hot water into the jacket until the required heating rate fell within the range of the heaters. By regulating the hot water addition in accordance with the indications of the Wheelco meter the temperature lag during the few minutes of surge could be practically eliminated.

A second problem was introduced by the water circulating pumps which proved to be an uncontrollable source of heat to the water jacket. Close mechanical coupling permitted most of the motor heat to flow to the pump and the circulating water. This effect was aggravated by the fact that the pumps were larger than required and had to be throttled to about one-fifth of normal capacity. As a result, the total energy from the pump and motor proved sufficient to sustain a water jacket temperature of 45°C against total thermel losses to the room. To compensate for this heat supply, copper cooling coils were installed in the water jacket, and with proper adjustment of cooling rate, the water temperature cycled through a 0.5°C range about once per minute.

Preliminary adjustment of the water jacket control system was made by heating the copper block to 30°C (the selected final temperature for all enthalpy change measurements) and then adjusting the Wheelco Controller to maintain a block-to-water-jacket thermal differential that would hold the block temperature constant. In preliminary tests and in subsequent rechecks during specimen measurements, the block temperature was held constant within 0.002°C for several hours. However, since the accuracy of this control was influenced by the room temperature and by the temperature and flow rate of the jacket cooling water, an ideally adiabatic condition was not always achieved.

3.2.3 Furnaces

Standard tube-furnaces were mounted, as shown in Figure 6, to swing in a horizontal plane above the calorimeters. They were modified by installation of two alundum tubes which projected from the furnace ends and intermediate stainless steel tube located in the midsection of the furnace to define the specimen heating chamber and promote temperature uniformity therein. The middle steel tube was 6 inches long and had one-half inch thick walls. The upper ceramic tube supported the specimen holder, and the lower one guided the released specimen into the calorimeter. The specimen holder, which was inserted from the top, included radiation baffles at the lower end, and another system of baffles was inserted from the lower end of the tube.

The specimen hanger consisted of two parallel metal rods mounted through a Transite plate at the top end and spaced at the lower end by the radiation baffle plates and ceramic insulators. The specimen was suspended from a loop of Nichrome wire fastened to the rod ends and was released by melting the wire by means of 110V A.C. applied to the support rods.

Power supply to the furnace was controlled by a Weston Celectray Controller actuated by a thermel located outside the furnace heating chamber but close to the heating element. A second thermel was inserted from the side into the heating chamber to sense the internal temperature; this thermel was connected through the switching system to the K-3 potentiometer.

Evaluation of the temperature of a specimen before the drop was necessarily an indirect process. At each furnace temperature, as determined by a particular setting of the Celectray Controller, the temperature of a dummy specimen was measured. The later was a solid replica of the hollow specimen capsule and was provided with a thermel well to receive a standardized Pt-Pt, Rh. thermel. When thermal equilibrium was attained, measurement (K-3 potentiometer) was made of both the dummy specimen temperature and the heating chamber temperature as detected by the second thermel mentioned above. Thereafter, in all enthalpy measurements made with that same setting of the furnace controller, the specimen temperature was assumed to be that previously measured for the dummy. Immediately before a specimen drop, the heating chamber thermel voltage was measured, and if a small temperature change was revealed, the assumed specimen temperature was corrected accordingly.

3.2.4 Specimen Capsules

The specimen capsules were cylindrical metal cups, 2 1/2 inches high and tapered from 1 3/8 inch O.D. at the top to 1 1/8 inch O.D. at bottom (Figure 2). The capsule cover included a central post with a transverse hole to take a wire bale by which it was suspended in the furnace.

On the basis of early recommendations, a first set of capsules was prepared from Inconel bar stock. However, one capsule leaked badly at a weld and others exhibited possible leaks. A second set of capsules was fabricated from Type 316 SS bar stock. The first one tested with a LiH specimen revealed small leaks through the bottom and lid. Since these surfaces were normal to the bar stock axis, it was inferred that the LiH dissolved slag stringers to make small channels through the wall. Subsequently, the bottom and lid surfaces were sealed by superficial melting with the Heliarc before use.

3.3 Specimens and Preparation

3.3.1 Sapphire Standard

Synthetic sapphire was purchased, in the form of split boules, from the Linde Division of Union Carbide and Carbon Corporation. It was broken into smaller pieces, washed and

dried, weighed, and sealed into a capsule. Comparatively elaborate procedures have been described for preparation of the sapphire as a thermal standard (Ref. 6) but they were deemed unnecessary in view of the general accuracy expected of these measurements.

3.3.2 LiH Specimens

Lithium hydride and lithium metal were purchased from Foote Mineral Company. The LiH had been crushed and graded under purified argon and finally packed under argon. Upon receipt here, the LiH was passed through sieves to eliminate the fines, and only the crystals of +10 mesh size were reserved for use. Chemical analysis by a dry method indicated a hydrogen content 97.6% of the stoichiometric value. Analysis for oxygen was not attempted because a reliable method was not available, and analysis for other contaminants, normally present in very small concentration, was not attempted because a significant influence on the thermal properties was not anticipated. Moreover, it seemed certain that the LiH would acquire, during the course of the measurements, a greater concentration of many contaminants than it contained originally.

The lithium metal was selected by Foote from analyzed stocks and packed under argon. Immediately before use the metal was cut and all surfaces were trimmed.

All capsule-filling operations were performed in the dry box under purified argon. The LiH and Li metal were weighed to 0.01g on a triple beam balance. The capsules were weighed, before and after filling, on an analytical balance as a check on the validity of weighings made in the dry box.

When the capsules had been filled with LiH and LiH-Li mixtures, the covers were pressed tightly into place and immediately upon removal from the dry box, were sealed by Heliarc welding.

Four capsules were prepared with contents as follows:

Capsule	LiH	Li	LiH	Li	Total Mols.
I	7.55g	0.0 g	100 mol%	0 mol%	0.944
J	6.77	0.75	88.9	11.1	0.953
K	6.02	1.31	80.1	19.9	0.940
L	5.26	1.98	69.9	30.1	0.941

3.4 Measurement Procedure

Enthalpy changes of the specimens were measured for the temperature changes from initial values ranging from 600 to 800°C, to the final calorimeter temperature of 30°C. Corresponding measurements were made with an empty capsule to evaluate its contribution to the total measured enthalpy loss by the encapsulated specimen. This can be computed from the known specific heat of the capsule material, but the method of direct measurement for each different furnace temperature has the advantage of incorporating at least partial corrections for systematic errors not amenable to convenient evaluation. One such is the loss of heat by the specimen while falling from the furnace into the calorimeter. Since the time of fall is very short, one may assume that heat loss from a filled capsule will be primarily from the capsule alone. Consequently, the data for an empty capsule enters into the computations performed on data for a specimen as a correction for that unevaluated error.

3.4.1 Preparation of Specimen and Furnace

The furnace temperature at each controller setting was determined with the dummy specimen and the furnace chamber thermel, as described previously. The specimen was then inserted and allowed to soak for at least 1 1/2 hours to attain thermal equilibrium. Immediately before dropping the specimen a measurement of the furnace chamber thermel was made.

3.4.2 Preparation of Calorimeter

The calorimeter required adjustment to a proper initial temperature such that a final temperature of 30°C was attained after specimen drop. Usually this involved cooling below room temperature. Small pieces of dry ice were used to cool the copper block while the water jacket was cooled by circulating tap water through the cooling coil, or for more severe cooling, by putting ice directly into the jacket water. Ample time was allowed for attainment of equilibrium. The ideal was a constant block temperature, but at the lower starting temperatures, a very slowly rising block temperature was the best compromise.

When all was ready, the calorimeter gate was opened, the furnace lower baffle was removed, the furnace was swung into place over the calorimeter, a switch was thrown to release the specimen. The furnace was immediately swung aside, and the gate was closed. Hot water was then poured into the water jacket to supplement the heaters during the first rapid temperature rise. When equilibrium temperature was approached, water supply to the water jacket cooling coils was started. When the point recorder indicated approach to equilibrium, measurement of the calorimeter thermopile output was made at 5 minute intervals with the K-3 potentiometer, and the values were recorded in millivolts. Measurement was repeated until the attainment of a stable level was evident.

3.5 Computations

3.5.1 Empty Capsule

Let K represent the calorimeter constant or heat capacity in Joules per millivolt as determined by calibration against the sapphire standard. ΔV is the change in millivolts of the copper block thermopile potential; Δt is the temperature change in degrees C of the specimen in cooling from the furnace temperature to the final calorimeter temperature. M is the weight in grams of the empty capsule; and C is the average specific heat of the capsule material over the range Δt.

Then the equivalence of heat gain and loss are expressed as follows:

(1) $K \Delta V = \Delta t M C$

(2) or $C = \frac{\Delta V}{\Delta t M} K$

For convenience, let $c = \frac{C}{K}$

(3) $c = \frac{C}{K} = \frac{\Delta V}{\Delta t M}$

The average specific heat of the capsule material, being thus expressed in terms of the calorimeter constant, has slightly different values for the two calorimeters.

Moreover, since the specific heat of the metal changes with temperature and the data from each drop includes uncorrected heat losses and other systematic errors, the empirical value of c changes with increase in the initial (furnace) temperature. Figure 12 is a plot of the values of c versus initial capsule temperatures. The greater scatter of values evident in the plot for calorimeter No. 2 is a consequence of troubles encountered in operating that equipment. The values of c used in subsequent computations were taken from the best straight line through the points.

3.5.2 Sapphire Standard

The sapphire standard was a composite of sapphire and its metal capsule. Therefore, it follows that:

(4) $Q + cMK\,\Delta t = \Delta VK$ or

(5) $Q = K(\Delta V - cM\,\Delta t)$ where Q is the heat lost by the sapphire to the calorimeter as a result of the temperature drop Δt. Q was evaluated from the relation:

(6) $Q = H_t - H_{30}$

(7) $= (H_t - H_0) - (H_{30} - H_0)$

and the relation (Ref. 6)

(8) $H_t - H_0 = 1.44798t - 1.6777 \times 10^{-5}t^2 - 460.915 \log \frac{t+273.16}{273.16}$

which is very accurate for values of t above 125°C and introduced about 0.1% error below 125°C.

In standardizing, equation (5) is used to evaluate K, the calorimeter constant. Q is computed from equations (7) and (8), ΔV and Δt are measured, M is the weight of metal in the sapphire-containing capsule, and c is a function of the specific heat of the capsule metal, as defined previously.

The values of K obtained for the two calorimeters are listed on the next page.

Calorimeter No. 1	Calorimeter No. 2
4658 J/mv.	4690 J/mv.
4678	4720
4682	4699
4669	Av. = 4703 J/mv.
4681	Av. dev. = ±17
4668	
4670	
4687	
4675	
Av. = 4675 J/mv.	
Av. dev. = ±7	

These average values for each calorimeter, respectively, were used in all the calculations described below.

3.5.3 Lithium Hydride Specimens

Equation (5) was used to interpret the data from measurements on the lithium hydride specimens. Q is the heat lost by the contents of the capsule, K is the calorimeter constant, the specific heat function "c" of the capsule metal was taken from the appropriate plot (Figure 12), M is the weight of the capsule alone, and ΔV and Δt are measured directly.

3.5.4 Typical Calculations

Recorded below are data and computations typical of measurements with the empty capsule, the sapphire standard, and specimen J, which contained the nominal 80-20 mol % LiH-Li mixture.

Empty Capsule:

(Wt. of capsule = 109.06g)
Furnace temperature 805.1°C
Calorimeter initial thermel voltage 20.676 mv.
Calorimeter final thermal voltage 30.598 mv. $\simeq$ 29.9°C

ΔV = 9.922 mv.
Δt = 805.1-29.9 = 775.2°C

$$C = \frac{\Delta V}{\Delta t M} K$$

$$= \frac{9.922}{775.2 \times 109.06} K$$

$$= 1.1636 \times 10^{-4} K$$

or $c = 1.1636 \times 10^{-4}$

Sapphire Standard:

Wt. of sapphire	70.1905g
Wt. of capsule	113.46g
Furnace temperature	647.9°C
Calorimeter initial thermel voltage	12.396 mv.
Calorimeter final thermel voltage	30.455 mv. ⇐ 29.7°C

$\Delta t = 647.9 - 29.7 = 618.2°C$

$\Delta V = 30.455 - 12.396 = 18.059$ mv.

From equations (7) and (8), Q for the sapphire is 46763 Joules.
From a plot of c vs t, (Figure 12) the value of c at 648°C is 1.15×10^{-4}

$Q = K (\Delta V - cM\Delta t)$

$46763 = K (18.059 - 1.151 \times 10^{-4} \times 113.46 \times 618.2)$

$= K (18.059 - 8.073)$

$= K (9.986)$

$K = \frac{46763}{9.986}$

$= 4683$ Joules/mv.

Specimen J

Weight of LiH 6.77g = 0.846 mol
Weight of Li 0.75 = 0.107 mol
Total contents 7.52g = 0.953 mol

Weight of empty capsule	114.44g	
Furnace temperature	702.3°C	
Calorimeter initial thermel voltage	11.377 mv.	
Calorimeter final thermel voltage	30.983 mv.	30.2C

$t = 702.3-30.2 = 672.1°C$

$V = 30.983-11.377 = 19.606$ mv.

c derived from the c vs. t plot (Figure 12) is 1.158×10^{-4} and K is the average value, 4674 J/mv.

$Q = K(\Delta V - cM\Delta t)$

$= 4674\ (19.606-1.158 \times 10^{-4} \times 114.44 \times 672.1)$

$= 4674\ (19.606-8.907)$

$= 4674\ (10.699)$

$= 50000$ J

$= \frac{5000}{4.185} = 11947$ cal.

$Q/\text{gram} = \frac{11947}{7.52} = 1589$ cal/g

$Q/\text{mol} = \frac{11947}{0.953} = 12642$ cal/mol

1589 cal/g = 1589 X 1.8 = 2860 Btu/lb.

3.6 Data and Interpretation

In Tables 1, 2, 3, and 4 are listed the results of enthalpy measurements of the LiH and LiH-Li containing specimens. The tables do not include the results of many measurements which were rejected (as explained later) because of excessive deviation from the general trend. All the values derived from earlier measurements made with calorimeter No. 2 were rejected on the basis of subsequent discoveries concerning the peculiar and unexpected characteristics of that apparatus. Data taken later with suitably modified technique correlated satisfactorily with that from calorimeter No. 1.

Since loss of hydrogen by diffusion was expected as the cause of a progressively increasing error, the measurements were not made in the order in which they are tabulated, i.e. in order of increasing initial temperature. Selection of temperatures was randomized in order to prevent the concealment of such an error in the influence of temperature. Although reweighing of the capsules after months of use revealed losses of a small fraction of a gram, this could readily be attributed to slight oxidation of the capsule and sloughing off of the oxide. The reasonably good agreement between early and later measurements made in the same temperature region indicates good retention of hydrogen. Moreover, since the ΔH_f value computed from our data for pure LiH corresponds with that obtained by Dr. H. E. Hoffman's group at ORNL, there is support for our belief that severe loss of hydrogen from the specimens did not occur.

In Figures 13, 14, 15 and 16 the enthalpy changes of the four specimens are plotted against values of t. In each case the data above and below melting point are assumed to define a straight line extending to the melting point. Actually, an "S" shape is evident through the melting range, and some curvature is to be expected for the solid and liquid enthalpy plots, but the range of temperatures explored is too short and the data insufficiently precise to justify more than an assumed straight line.

A consistent peculiarity in the data from all four specimens is the apparent abrupt rise in the enthalpy curve near 800°C. The data are not easily discredited since it was taken rather recently, after technique was perfected and after the major apparatus refinements had been made. The contribution of heat of dissociation of LiH is recognized, but a gradual effect seems more probable than what appears here. An extension of measurements into higher temperature regions is required to verify the apparent change in course of the curve.

In estimating the heat of fusion, the melting temperature 688°C was assumed for all four specimens despite the evidence of a somewhat lower melting point in our data. According to C. E. Messer, (Ref. 2) pure LiH melts at 688°C and in LiH-Li mixtures containing less than 95 mol % LiH the B phase melts at 685°C. The error introduced by using 688° is negligible.

By the method of least squares, expressions relating enthalpy change to temperature were derived for the solid and liquid states of the four specimens. The equation has the general form:

solid: $H_t - H_{30} = -333 + 1.84t$

$H_t - H_{30} = A + Bt$

in which $H_t - H_{30}$ is the enthalpy change involved in temperature change from t°C to 30°C; A and B are constants. For the solid, the range of t is 600 to 680°C; for the liquid 700 to 800°C. In Tables 5A and 5B are recorded the values of A and B, the average deviations of observed from calculated enthalpies, the calculated enthalpies for solid and liquid at 688°C, and the heats of fusion. The heats of fusion (ΔH_f) and specific heats (B) are plotted against specimen composition in Figure 17.

Our value for heat of fusion of pure LiH (659 cal/g) may be compared with 694.4 cal/g reported by H. E. Hoffman (2) and 625 cal/g reported by Wilson, Boehn, and Cooper (Ref. 3). Hoffman also reported enthalpies as follows:

For solid LiH in the range 100°-650°C

$$H_t - H_{30} = -32.17 + 0.914\ t + 71.30 \times 10^{-5} t^2$$

For liquid LiH in the range 700°-900°C

$$H_t - H_{30} = 291.47 + 1.988t - 6.35 \times 10^{-5} t^2$$

When these two equations are converted into expressions for an assumed straight line function in the range 600-680°C and 700-800°C respectively, they become:

liquid: $H_t - H_{30} = 321 + 1.90t$

which are to be compared with our expressions:

solid: $H_t - H_{30} = -484 + 2.087t$

liquid: $H_t - H_{30} = 398 + 1.762t$

4.0 Thermal Conductivity

4.1 General Considerations

Thermal conductivity of LiH was to be measured for both the solid and liquid states at temperatures near the melting point. Selection of the particular method and design of the apparatus was dictated by several considerations. First, the budget imposed on the project compelled adoption of a single apparatus for all the measurements, despite the realization that the solid and liquid states entail quite different problems. Second, the lack of the extensive background experience and of the specialized precision equipment required to undertake absolute measurements necessitated the adoption of a comparative method. Third, the prolonged containment of LiH (probably mixed with Li metal) at temperatures near 800°C could be achieved only in austenitic type stainless steel with good welding characteristics, resistance to oxidation, and low hydrogen permeability.

A glazed ceramic or glass apparatus is preferable to metal with respect to hydrogen containment and to thermal conductivity (being comparable with that of the specimen LiH) but such materials are severely attacked by LiH and must be avoided. Type 304 SS was selected as a reasonable compromise of the desired properties with commercial availability of the stock required and the problems anticipated in having the apparatus fabricated.

When the material to be measured is solid, several general types of apparatus design may be considered. One may choose the flat wafer with a transverse gradient, or the cylindrical annulus, or the spherical annulus, and the thermal gradient may be static or dynamic. However, the measurement of liquid conductivity necessitates a design that prevents convection. Consequently, the thermal gradient must be vertically downward and static. The specimen must therefore take the shape of a horizontal wafer with minimum thickness to reduce convection tendencies and maximum diameter to minimize edge effects. In this instance, namely, the containment of LiH in a material roughly ten-fold as conductive, perturbation of the thermal pattern at the specimen wall must be severe, and the demand for thinness and large diameter is particularly emphatic. Therefore, thermels within the specimen should be omitted and temperatures and gradients within the specimen would be inferred from the thermels located in the heat meters above and below the specimen.

However, the specimen thermels could not be eliminated because some of the information necessary to justify this design was not available or was unfavorable. It was not certain that the specimen chamber would fill completely, or that the LiH-metal interface would develop insulating layers, or that convection could be prevented, or that cracking of the solid would disturb thermal continuity. It seemed likely that complete fill and good contact with the upper surface could not be maintained upon freezing. Consequently, temperatures and thermal gradients in the LiH must be measured, not inferred; thermels must be located within the specimen chamber. (Thermels attached to the specimen chamber walls, a practice sometimes adopted, could not be used because of the greatly different conductivities of stainless steel and LiH.) In order to minimize distortion and displacement of the thermels by melting and freezing LiH, the thermel wells were extended horizontally through the chamber and secured to the wall at each end. The smallest stainless steel tube practical from the aspects of rigidity, wall thickness, internal diameter and welding at the chamber wall, was of 1/16 inch I.D. and 1/8 inch O.D. With three such thermel well tubes through the chamber a total steel thermal path of roughly 3/8 inch was created through the LiH. In a chamber one-inch high, the steel thermal path therefore represents about 35% of the total thermal path. Moreover, the measuring thermels are located at the sites of the thermal disturbances created by this material discontinuity. To reduce this source of error by increasing the chamber height was not practical because that would necessitate a proportionate increase in diameter, which would involve a great increase in the mass of the upper heat meter to be supported by the specimen wall and an increase in length of the thermel wells with consequent decreasing rigidity. Furthermore, an increase in specimen height (say three-fold) would entail a proportionate increase in the general vertical dimensions of the apparatus if the desired temperatures and gradients were to be preserved.

4.2 Specific Design of Apparatus

The specific design adopted is represented schematically in Figure 19 and is presented photographically in Figure 8. It is a 3-inch diameter cylinder 11 inches high containing a 1-inch-high specimen chamber at mid-height. It is surrounded by a guard-ring (also Type 304 SS) which is, in turn, enclosed within a ceramic cylinder bearing 8 nichrome wire heaters in spiral grooves in the outer surface. A flat Nichrome wire heater, embedded in an alumina form rested atop the central cylinder and

provided the heat for an axial downward thermal gradient, while the 8 peripheral heaters provided a degree of control over guard-ring temperatures at the various levels. The entire assembly was mounted at the center of a vertical Transite cylinder (18 inch diameter) which was finally filled with loosely packed vermiculite for thermal insulation. (Figures 9 and 10). Escape of heat from the bottom was regulated by varying the packing of insulation directly below the central assembly.

Following are more specific details:

4.2.1 Central Cylinder

The central cylinder was fabricated by joining two solid pieces (the top and bottom sections) to a piece of tube of 1/16 inch wall thickness. The upper cylinder was first bored to provide a filling hole, angling from the top center toward one side, then vertically downward into the specimen chamber. After joining the pieces, all external beads, lumps, and bulges from the welding operation were removed by lathe-work.

A melting-and-filling reservoir 2 inches in diameter by 7 inches high was joined to the cylinder top by a 4-inch high, 1/4 inch I.D. tube and provided at the upper end with a 1 inch diameter fill-tube. The latter was closed by a threaded cap with tapered metal-to-metal seal to protect temporarily against atmospheric contamination before the cap was sealed permanently by welding. From the top of the cap extended a stainless steel tube ending in a valve that was ultimately connected to a vacuum system and to a hydrogen gas supply.

For the measurement of thermal gradients, radial holes (1/8 inch diameter) for thermels were drilled to the center in both upper and lower sections of the central cylinder at 1 inch intervals, beginning 1/8 inch from the specimen cavity surface. At the same levels, very shallow holes were drilled for thermels to measure surface temperatures.

At three levels (mid-height, and 1/8 inch from top and bottom) straight tubes (1/16" I.D.) for thermels were passed through the specimen chamber. To avoid the maximum thermal distortion that would result from locating all three in the same vertical plane through the specimen axis, the upper and lower tubes were displaced 120° from the middle one, and all three were displaced horizontally to by-pass the specimen axis by 1/4 inch (Figure 19). The tube mid-points, at which the thermal junctions were to be located, were thereby not positioned one directly above another, but were still reasonably far away from the specimen chamber sidewall.

The entire cylinder was joined by welding to a circular base, the top surface of which was designed to support and locate the guard ring and guard heater cylinder co-axially with the central cylinder. The base rested, in turn, upon a 2 1/4 inch-high stainless steel ring to support the entire assembly above the inclosure floor.

The guard ring was a cylindrical tube of 304 SS with 1/4 inch thick wall, and 3 1/2 inch I.D., thus providing a 1/4 inch air-gap between it and the specimen cylinder surface. At mid-height, corresponding to the specimen chamber location, the wall thickness was reduced to 1/16 inch to make the downward thermal gradient in the guard ring conform more closely to that expected in the specimen cylinder because of the abrupt change from steel to LiH to steel.

Thermel wells for measurement of the inner surface temperature were drilled radially almost through the guard ring wall at levels corresponding with placement of the specimen thermels in the upper and lower heat meter sections. Through-holes were also drilled for thermal leads from the interior and surface of the central cylinder.

4.2.2 Thermels

Thermels were prepared from chromel and alumel wire (24 gage), calibrated and supplied by Hoskine Mfg. Co., Detroit. The three intended for the specimen chamber were butt-welded in a condenser discharge device, insulated by 1/16 inch O.D. alundum spaghetti and passed through the

thermel tubes, the bead located at midpoint and the leads projecting from opposite ends. All other thermels were prepared by twisting the wire ends together and welding by an AC arc-to-mercury under a quenching layer of silicone oil. Leads were inserted through lengths of double-hole alundum round insulator sufficient to extend beyond the region of high temperature. Vinyl plastic spaghetti was used to continue insulation to the cold junctions submerged in an ice bath. The latter thermels were inserted into the blind thermel wells provided in the upper and lower heat meter body and surface, and in the guard ring. All leads were passed upward in the space separating the guard ring outer wall from the guard ring heater. Nichrome wire bands were wrapped around the thermel leads and guard ring at appropriate intervals to hold the thermal beads in contact with the thermal well bottoms.

All thermels were connected to the L & N Type K-3 Potentiometer through a double-pole multi-position switching system, so that each thermel was electrically independent of all others. Several preliminary tests indicated that the addition of electrical guarding of the thermal circuits had a negligible influence on the potentiometer measurements and a guard system was not provided.

4.2.3 Heaters and Power Supply

The guard heater was made from a section of alumina furnace tubing of 5 inch I.D., 1/4 inch wall thickness, with external spiral grooves (3 per inch). Spiral-wound Nichrome 5 heaters were wound in the grooves making 8 heater sections to provide 4 equally spaced sections for the upper heater, 4 for the lower, with a slight overlap of numbers 4 and 5 into upper and lower parts of the specimen region.

The specimen-top heater was made by embedding spiral-wound Nichrome wire in alumina cement in grooves milled into the surface of a slab of alumina. The later was made as a disk large enough to cover the specimen cylinder and guard ring tops and was slotted radially to accommodate the central fill tube. Above this heater was mounted the reservoir heater--a 2 1/2 inch I.D. spiral grooved alumina furnace tube 12 inches high, wound with Nichrome wire. A thermel was located inside the reservoir heater and another rested on the specimen-top heater.

Electrical power to the ten heaters was controlled by 10 Variac autotransformers, all connected to the output of a large Powerstat autotransformer, which in turn was fed by a 5KVA Sola Constant Voltage Transformer. Thus, each heater was controllable individually while general changes in temperature could be made by adjustment of the master powerstat.

4.3 Procedure

4.3.1 Filling and Sealing Apparatus

After fabrication and assembly of the central specimen cylinder, it was tested for leaks by the helium mass spectrograph. One weld imperfection was discovered and corrected. The cylinder was also radiographed to insure proper location of thermel wells, and absence of significant voids in the heat-meter sections.

The entire central cylinder, was placed in a vacuum-purge dry box and pumped to less than 0.1 micron pressure. The box was back-filled with high-purity argon gas passed through titanium sponge getter at about 980°C. The melting reservoir was then filled with crushed LiH of 10 mesh size. The threaded cap was tightened securely on the reservoir, the valve at the top was closed and after removal of the entire assembly from the dry box, the cap was welded for a permanent seal.

4.3.2 Operating Procedure

After mounting the specimen cylinder, guard ring, and guard heater, installing the thermels, and insulating as previously described, the gas tube valve was connected to a pipe and valve system which permitted alternate evacuation and back-filling with purified hydrogen. The cycle was repeated several times to insure complete replacement of the argon gas by hydrogen. Hydrogen from a gas cylinder provided with a low-pressure diaphragm control valve was passed through three small De-Oxo units and an alumina drier. There was also an oil-filled bubbler to permit hydrogen escape when the interior pressure exceeded atmospheric pressure by more than the head of oil.

The melting reservoir was originally charged with about 50 percent more LiH than that required to fill the specimen chamber and connecting tube. Therefore, as long as the LiH supply remained fluid, a complete fill of the specimen chamber was possible despite changes in volume or density in the chamber.

The original plan in operating the apparatus was to heat the central cylinder above the melting temperature of LiH first, then raise the reservoir temperature above the melting point. All LiH in the system was then to be maintained molten until all measurements on the liquid were completed. Then by carefully controlled reduction of temperatures, freezing was to progress upward through the specimen chamber. Once complete solidification had occurred, remelting was not to be attempted because of the danger of bursting the apparatus. However, soon after beginning operations a general power failure which endured for several hours caused freezing of the entire specimen chamber contents. Subsequent return to the original operating temperatures occurred without damage detectable at that time.

When the desired temperature level had been attained and chamber fill was presumed accomplished, the guard heater controls were adjusted to develop a constant thermal gradient through the heat meters and uniform temperatures in the heat meter center and surface and guard ring at each horizontal level. After every change, many hours were allowed to elapse and measurements were then made at intervals of several hours to insure the attainment of practical equilibrium.

4.3.3 Performance of Apparatus

During a period of approximately two months the apparatus was maintained at, or above, the melting point of LiH, i.e. 688°C. Following is a chronologue:

May 19 - Assembly was completed; all thermocouples were measured for malfunction and uniformity at room temperature. Heating of guard trimmers and top heater was begun.

May 24 - Reservoir temperature was raised above LiH melting point and the chamber was presumed filled.

May 25 - Stability was achieved and good data were recorded.

June 3 - Thermel #33 (lowest in specimen chamber) failed.

July 13- Thermel #16 (at lower heat meter surface directly below specimen chamber) failed. Measured voltage became so great that only electrolytic action seemed a tenable explanation. A leak of LiH was thus indicated.

June 24- Thermel #5 (directly above center of the specimen chamber) became erratic and later failed.

July 14- Thermel #31 (uppermost in specimen chamber) became unsteady and failed.

July 21- Power was disconnected and the apparatus was cooled.

Considerable data were recorded after these thermel failures because earlier measurements had provided a reasonable understanding for interpolation of curves on the basis of the remaining thermels.

Beginning July 17, preliminary to ending all measurements, the temperature was decreased in stages well below the LiH melting point and data were recorded for the solid material. After cooling to room temperature, a final measurement of all surviving thermels was made to check for gross inequalities; minor variations were observed, but no glaring differences.

4.3.4 Final Examination of Apparatus and Contents

Upon dismantling the assembly, an attempt was made to remove the thermels intact for a high-temperature comparison against a standard, but most of them in critical locations were destroyed in the attempt. LiH leakage had occurred evidently at one end of the lowest thermel tube projecting through the LiH chamber. The leaked material had migrated over the outer surface of the specimen cylinder and the contiguous inner surface of the guard ring (Figure 11),

and a solid deposit of several millimeters thickness had accumulated about the site of leakage. The ceramic insulators of nearby thermels were attacked and partially disintegrated. The failure of thermels was evidently attributable to this one leak of LiH.

The specimen chamber and reservoir were opened with a pipe cutter. In the chamber, the LiH was of lavender color and filled the chamber completely except for a slight void at the upper surface. The thermel tubes were not distorted and were completely embedded in adherent solid material. The bottom and side metal surfaces were clean, but appeared slightly dull, as though etched. The top metal surface was coated by a thin brown layer, which gradually became moist after exposure to air. This might have been Li_3N, but a test with water failed to reveal a detectable odor of NH_3. Any more critical test for nitride was precluded because the amount of material was limited. Wet method qualitative tests performed on a water solution of pieces of the LiH revealed only ferric ion; chromium and nickel were not detected.

Analysis of the LiH for hydrogen by thermal decomposition in the presence of tin indicated substantially stoichiometric LiH composition--a greater hydrogen content than that observed in any of the specimens of commercial LiH tested. Actually, the analytical data, including a blank correction, yielded a percentage of hydrogen slightly greater than the stoichiometric maximum, but this is probably the consequence of an inadequate blank correction.

Analysis of another specimen for Li content by conversion to Li_2SO_4 revealed a lithium content almost exactly stoichiometric.

The apparent purity of the LiH was surprising in view of the leak to air which had occurred, evidently, relatively early in the period of measurement. Had the leak not occurred, the anticipated loss of hydrogen by diffusion through the chamber walls, compensated by hydrogen supplied principally by diffusion down a long route through the reservoir contents and connecting fill tube to the chamber, was expected to result in a net depletion of hydrogen from the chamber. The persistance of near-stoichiometric purity during most of the three-month period was attested by the data which, with one

exception, indicated the presence of only one liquid phase. According to the phase diagram for Li-LiH, material containing less than 95 mol % LiH forms two liquid phases above 685°C. Consequently, it seems that the hydrogen content was maintained at more than 95 mol %.

The melting reservoir contained very little LiH. The fill-hole at the bottom was not covered but a small quantity was found bridged across the reservoir at about mid-height. Unlike the specimen chamber contents, this LiH was brown in color. Wet qualitative tests applied to specimens also revealed only iron; chromium and nickel were not detected. Hydrogen content was comparable with that of the specimen chamber contents.

Absence of the intended reserve of LiH in the reservoir is attributable to progressive losses through the leak and to contraction of material in the specimen chamber during final solidification. Thermel measurements and thermal patterns indicated that the chamber usually remained completely filled except when containing solid only.

4.4 Data and Interpretation

4.4.1 Recording and Plotting of Data

As a convenience in interpreting the thermel voltages, they were recorded on a data sheet (Figure 20) arranged to resemble the relative orientation of thermels in the apparatus. The axial heat meter thermels were numbered 1-10; the cylinder surface thermels 11-20; the guard ring thermels 21-30. Those through the specimen chambers were 31, 32, 33. Number 35 was located just above the specimen top heater; number 36 was placed to monitor the melting reservoir temperature. At the right edge were recorded the settings of the main powerstat and the Variacs supplying the individual heaters.

From each such set of data, a plot of thermal gradients was prepared. (Figures 21, 23, 24 25). The voltages of the axial thermels (1-10) and the specimen thermels (31, 32, 33) are plotted against their vertical distances from #1 thermel.

At the right edge of the paper the thermel voltages are plotted in three vertical columns--central, surface and guard ring--with those at corresponding levels in the apparatus joined by lines.

In an ideal situation, the axial gradient curves through upper and lower heat meters would be straight lines of identical slope and that through the specimen would be a straight line meeting the upper and lower curves at the specimen-metal interface. The plot at the right would form a series of horizontal straight lines separated by equal distances in the heat meter sections. Any digression from the latter pattern is indicative of radial heat transfer, which should be avoided.

It is apparent that such an ideal was not attained. Just above the specimen chamber, the surface temperature was lower than that of the center and the guard ring, indicating heat escape down the chamber wall. As a result, the surface temperature below the chamber was high. The central temperatures below the specimen were low because of an inadequately controlled heat loss from the bottom.

Because temperatures of the heat meters could be measured only at the surface and center, the magnitude of radial gradient effects at the central region could not be measured directly. However, consideration of the vertical gradient patterns suggested that the edge effects were very much attenuated near the center.

After much experimentation with the heater controls, the thermal pattern plotted in Figure 18 was accepted as the best attainable. The chamber was evidently filled with molten LiH; the guard heaters (other than the lowest two) were at similar power levels. In the upper section, the gradient was a straight line, and the specimen gradient intersected both upper and lower gradient lines at the specimen interface. The high value of number 4 thermel was observed consistently and could not be explained in terms of surrounding temperatures. It could be brought into line only by severely distorting the general thermal pattern. Therefore, the upper gradient plot was based on the voltages measured for thermels numbers 1, 2, 3, and 5. The same high value of number 4 thermel voltages was observed consistently in all good stable patterns, and consequently thermel number 4 was omitted in the determination of the upper heat meter vertical gradient.

4.4.2 Computations

Conductivity of the specimen is computed as follows: The heat flux near the cylinder axis was assumed to be constant through the upper heat meter and the specimen. In each material, the flux, thermal conductivity, and thermal gradient bear the relation:

(9) Flux = $q/A = -k \frac{dt}{dx}$ where q = calories per second

A = cross sectional area

k = thermal conductivity

t = temperature in °C

x = axial distance in cm.

If the values for the heat meter and the specimen are designated by the sub-letters m and s respectively,

(10) $(q/A)_m = (q/A)_s$

(11) $-k_m \left(\frac{dt}{dx}\right)_m = -k_s \left(\frac{dt}{dx}\right)_s$

Inasmuch as the gradients are straight lines, the equation simplifies to,

(12) $k_s = k_m \frac{\Delta t_m \Delta x_s}{\Delta t_s \quad x_m}$

The axial distances used in meter and specimen were 4 and 1 inches, and the relation therefore becomes:

(13) $k_s = k_m \frac{\Delta t_m}{\Delta t_s} \times 1/4$

Values of Δt were measured and values of k_m were obtained from a plot of the following values reported (Ref. 5) for Type 304 SS at various temperatures.

t°C	k_m
500	0.051 cgs.
700	0.058
900	0.064

Application of equation (13) to the data is illustrated on each of the Figures 21, 23, 24, 25.

4.4.3 Data for Molten LiH

In all, about 120 sets of thermel measurements were obtained from the apparatus. Of these, the first 17 sets were preliminary. Many of the later sets were rejected because of thermal instability, or because the thermal pattern was evidently distorted. Those selected as worthy of consideration are summarized in Table 6 for molten LiH, and in Table 7 for solid LiH.

In Table 6, the data numbered 55 to 65 are believed to be the best obtained. The specimen average temperature was being advanced slowly from 711 to 772°C; the patterns were stable and were as nearly isothermal horizontally and linear vertically as could be achieved. The computed conductivity for the molten LiH declined from 0.0112 to 0.0094 (cgs).

After the taking of datum number 65, it was believed, in view of thermocouple losses and the danger of protracted containment of the LiH that the establishment of alternative thermal patterns should be attempted. Accordingly, the reduction of radial gradients above and below the specimen chamber was attempted by decreasing the power to guard heaters 3 and 4, and increasing the power to guard heaters 5 and 6. A general change in the thermal pattern resulted and the computed conductivity for molten LiH dropped to 0.006 (cgs). However, the thermal pattern became distorted and unacceptable in several respects and the computed values of conductivity are therefore not reported. With datum number 85, all controls were returned to the settings in effect in datum number 56. The thermal pattern established was slightly different from that of number 56, but the computed value of conductivity is similar.

Summarizing therefore, the apparent best value for molten LiH at 717°C is about 0.0103 cal cm^{-1} deg. C^{-1}, sec^{-1} with a slight reduction in value as the temperature rises to 770°C.

4.4.4 Liquid-Liquid Two-Phase System

Figure 23 presents a type of thermal pattern observed early in the sequence of measurements (datum number 23) when the specimen was near 800°C. Immediately prior to the establishment of this pattern, the escape of considerable hydrogen through the bubbler (about 5 inches head) occurred. The thermal pattern endured for several days and was therefore regarded as a truly stable situation and not merely transitory. Evidently the specimen had separated into two phases, the upper one having a conductivity nearly that of the stainless steel, and the lower one similar in conductivity to molten LiH. The phase diagram for the Li-LiH system (Figure 22) describes the establishment at 800°C of two liquid phases when the mol percent of LiH has declined below 90. Of the two the lithium-rich alpha phase should have the lower density and higher conductivity.

At the upper metal-specimen interface (Figure 23) there is a thermal discontinuity separating the upper heat meter gradient from that determined by the upper two specimen thermels. Since that was not observed in any other instance for molten LiH, and since the discharge of hydrogen had occurred, it is assumed that a trapped layer of hydrogen gas was interposed between the specimen and upper chamber surface.

This interpretation is, of course, tentative. The only evidence was that furnished by the thermels. During the many weeks of continued observation, a similar pattern was not again established. This may be due to a subsequent replacement of the original bubbler which increased the head of oil from 5 inches to 16 inches. Thereafter, the escape of more than a few bubbles of hydrogen was not observed.

4.4.5 Liquid-Solid Two-Phase System

A third type of thermal pattern is presented in Figure 24. The chamber evidently contained molten LiH above a layer of solid LiH, which apparently occupied the lower two-thirds of the chamber. The thermal gradient curves drawn from the metal-specimen interfaces through the thermel points intersect at about 687°C. As indicated

in the figure, the computed conductivity of the solid LiH is 0.0172 cal cm^{-1} deg C^{-1}, sec^{-1} and that for the liquid is 0.00783. The low value for the liquid is attributable, at least partially, to the error involved in extrapolating from two closely spaced points.

In Table 7 are summarized the conductivities of solid LiH (and liquid LiH in several cases) as derived from partially solidified specimens. The temperature at which the liquid and solid gradient curves intersect is also listed. In the series of data numbered 43 to 52, that temperature is 687°. The other low values (629°) and the higher value (695°) may be indicative of thermal instability or of a non-uniform depth of solid in the chamber.

4.4.6 Solid LiH

Figure 25 presents the type of thermal pattern observed consistently when the entire chamber was below the melting temperature and therefore contained only solid LiH. Evident separation of the specimen from the upper heat meter surface caused a discontinuity in the gradient curves at the upper interface. At lower temperatures, as observed immediately before final cooling of the apparatus, the thermal discontinuity became progressively greater--probably because of an increasing gap between the metal and the shrinking solid.

Although its significance is very doubtful, the conductivity of solid LiH was computed from Figure 25. The value, 0.0142 cal cm^{-1} deg C^{-1} sec^{-1} is lower than that recorded in Figure 24 for the solid covered by a liquid layer.

4.4.7 Comments

The conductivity values for all-liquid and for the liquid-solid states possess merit because the specimen chamber was then completely filled. The values are probably high because, primarily, of the gradient-distorting influence of the three specimen thermel tubes. The data for the liquid-solid system provide relative values for the solid and liquid states, and thereby establish a bridge to the published values for solid LiH.

Thus the values for solid LiH (Ref. 1), if extrapolated as a straight line to 688°C, indicate a possible conductivity near the melting point of 0.005 to 0.007 cgs units. The values for solid LiH derived from the present measurements are roughly three times as great. If the validity of linear extrapolation of the values from Ref. 1 into the melting range is accepted, then one might interpret the three-fold difference in values as an indication of the magnitude of thermal distortion effects on our data. The conductivity values computed from our data are therefore submitted as tentative. One significant consequence of the present endeavor is the clarification of several important aspects of apparatus design for LiH conductivity measurement. They are discussed in Section 6.2.

5.0 Solidification of LiH

The experience acquired in working with LiH and LiH-Li mixtures has not elicited anyunforeseen characteristics relative to its solidification. The pure molten LiH is a very mobile fluid which flows into and fills readily all available cavities in a system. Metallic surfaces are chemically cleaned by molten LiH and good liquid-to-metal interfacial bonds are formed. Upon cooling, the LiH crystallization begins at the cooled interface and progresses outward. Since freezing occurs with about 15% volume decrease, shrink cavities tend to form, but with proper control of direction and rate of cooling, cavity development may be minimized.

After complete solidification of LiH the contraction that occurs with cooling to ordinary temperatures causes cracking near exterior containing walls. Generally this cracking is in the LiH and does not disrupt the LiH-metal wall bond. The bulk of solid LiH can usually be removed easily from a metal container, but a thin layer of tightly adhering LiH remains on the walls. When unsupported tubes pass through a chamber containing LiH, which is melted and frozen, the forces of contraction and adhesion cause distortion of the tubes, and in severe cases, partial crushing of the tubes has been observed.

When the LiH is diluted with Li metal, the freezing range is extended and a lower melting Li metal alpha phase tends to segregate from the higher melting LiH beta phase. Shrink cavities developed by freezing of the beta phase tend to be filled with the alpha phase. In a typical case, a cylindrical slug of LiH-Li material, removed from a test capsule after melting and freezing, was found to consist of a brittle cylinder of LiH with a deep central shrink

pipe which was completely filled with the softer Li metal. In any particular instance, the filling of shrink cavities by Li metal will be limited by the composition of the LiH-Li mixture present.

With increasing Li metal content, freezing and subsequent cooling was attended by less cracking, evidently because of greater plasticity of the solid with greater Li content. It was also observed that adhesion to the metal walls was not as tenacious when a large proportion of Li metal was present.

6.0 Recommendations

6.1 Enthalpy Measurements

There were several sources of difficulty in operating the calorimeters--all were extraneous to the fundamental design. Calorimeter No. 1 performed as expected; No. 2 was quite different in one important respect. Upon injection of a quantity of heat, the No. 1 thermopile voltage rose to a maximum within five minutes and remained constant. In a similar test, No. 2 thermopile rose to a maximum and then slowly dropped to a slightly lower constant value, the entire change requiring about one half hour.

Subsequent to discovery of this difference, a proper readjustment of the water jacket temperature control of No. 2 and continuation of thermel measurements to attainment of the constant plateau value brought the data from No. 2 into much closer agreement with that from No. 1.

The odd performance of No. 2 calorimeter block may well have been due to voids in the copper stock, discovered during fabricating operations. At that time the decision was made to use the copper stock, with its imperfections, rather than incur the long delay involved in procuring and machining new material.

A second problem was introduced by the use of water circulation pumps of excessive capacity. As a result, it was necessary to throttle the water flow, and the energy transmitted to the water jacket was sufficient to maintain its temperature at about 45°C. Since a final calorimeter temperature of 30°C had been selected, it was found necessary to install cooling coils in the water jacket. The preferable remedy is use of pumps of the minimum capacity, constructed to provide the minimum transmission of motor heat into the circulated water.

A third problem developed as the seasons progressed from spring to summer. At first, the preliminary cooling of the calorimeter was accomplished easily, but during the summer months, the tap water temperature became too warm for use. It was then necessary to add ice to the jacket water, and it was extremely difficult to attain temperature constancy in the jacket and copper block under these conditions. One possible solution was the selection of a higher temperature of reference; for example, 45°C rather than 30°C. A better alternative would be the provision of a refrigerated water supply.

Another problem was the very slow transfer of heat from the sapphire- containing capsule to the calorimeter--the time for attainment of thermal equilibrium was usually greater than one hour. Evidently the degree of thermal contact between the capsule wall and the rather large chunks of sapphire within was too low. The performance would be improved by crushing the sapphire to smaller average particle size to increase the sapphire-metal contact area.

6.2 Conductivity Measurements

Probably the most significant information derived from the attempt to measure conductivity is that the LiH purity can be maintained, despite diffusion loss of hydrogen, by a slight overpressure of hydrogen gas, and that there is no significant thermal barrier established at the LiH-steel interface. If another attempt were made to measure conductivity, the thermels through the specimen would be eliminated and the apparatus diameter would be doubled, at least. The thermal gradient of the specimen would then be inferred from measured gradients in the upper and lower heat meters. Measurement of the liquid single phase system should present no serious problem. However, interpretation of data for the solid-liquid system would probably require a stepwise descent through the melting range and a graphical extrapolation of the data to the hypothetical ideal of complete filling of the chamber by solid LiH.

7.0 Acknowledgements

Collaborators in this project were: David P. Laverty, Research Metallurgist, who assisted in designing the conductivity apparatus and carried the major part of the burden of constructing and operating it; and Vincent Timpano, Technician, who made the many calorimetric measurements.

We are indebted to Dr. H. E. Hoffman and J. W. Cook of Oak Ridge National Laboratory, who very generously supplied us with complete plans for the calorimeters and much valuable advice concerning the measurements to be made.

8.0 References

1. A Survey Report on Lithium Hydride
E. F. Messer
N.Y.O. 1960

2. Private Communication
J. P. Murray at Oak Ridge National Laboratory, 1960.

3. Determination and Analysis of the Potentialities of Thermal Energy Storage Materials
H. W. Wilson, K. W. Boehm, W. J. Cooper
ASD Tech. Report 61-187 (025 ± 5%)

4. Measurements of Thermal Properties
I. B. Fieldhouse, J. C. Hedge, J. I. Lang
WADC Tech. Report 58-274

5. Metals Reference Book
C. J. Smithells
Interscience Publishers
2nd Ed. 1955

6. G. T. Furukawa, et. al.
Thermal Properties of Al_2O_3 from 0° to 1200°K
J. Bur Research of N.B.S. 57, 67 (1956)

9.0 Bibliography

Lithium: Heat Content from 0 to 900°, Triple Point and Heat of Fusion, and Thermodynamic Properties of the Solid and Liquid.
T. B. Douglas, et. al.
J. A. Chemical Society 77, 2144 (1955)

Thermal Conductivity of Liquid Sodium and Potassium
C. T. Ewing, J. A. Grand, R. R. Miller
J. A. Chemical Society 74, 11 (1952)

Fused Salt Thermal Conductivity
W. R. Gambill
Chemical Engineer, p. 129, August 10, 1959

Apparatus for Measuring the Thermal Conductivity of Metals
S. T. Zegler, M. V. Nevitt
ANL 5611

APPENDIX I: FIGURES

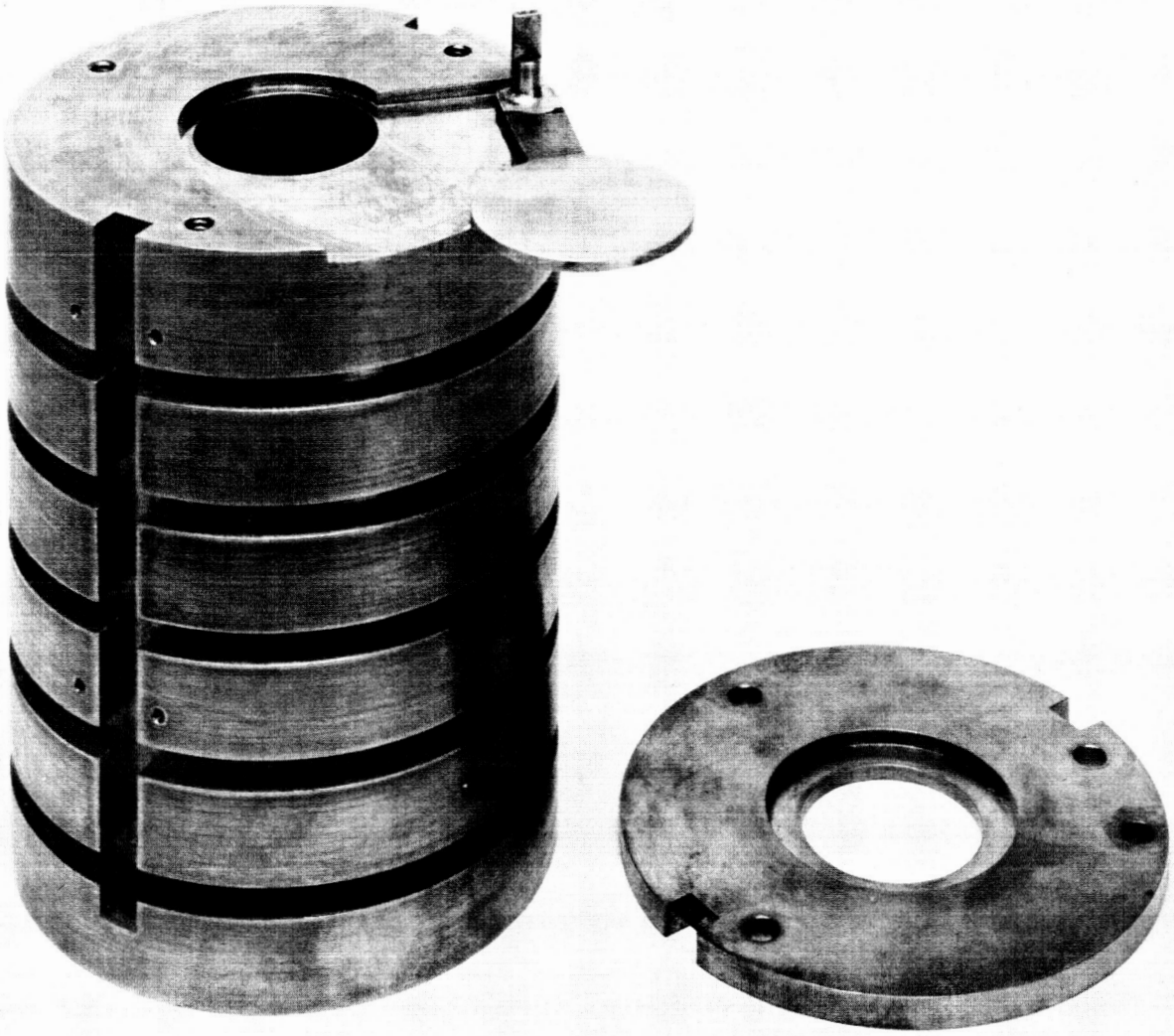

Figure 1. Copper block, gate, and cover.

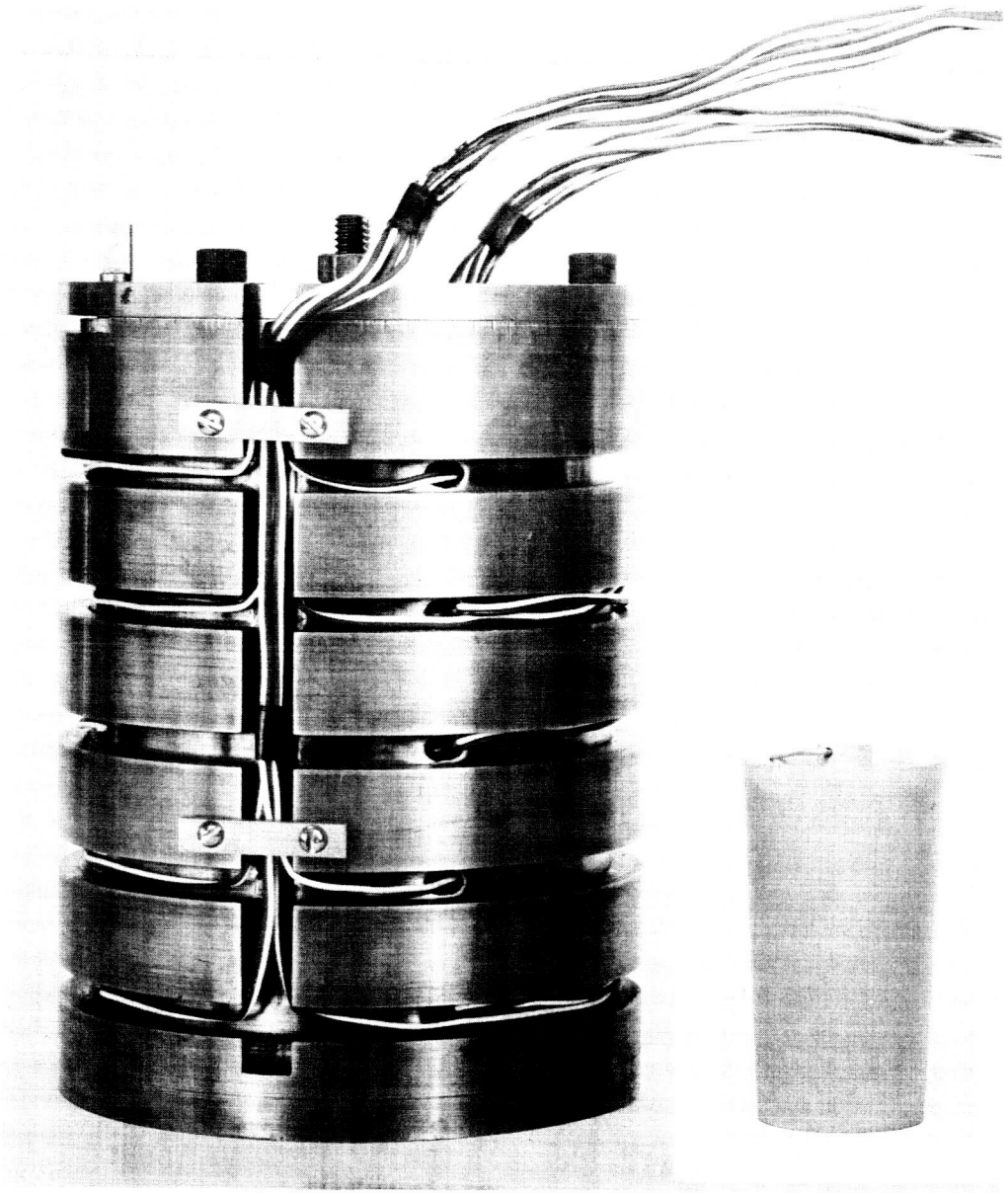

Figure 2. Copper block with thermels installed.
(Insert: Specimen Capsule)

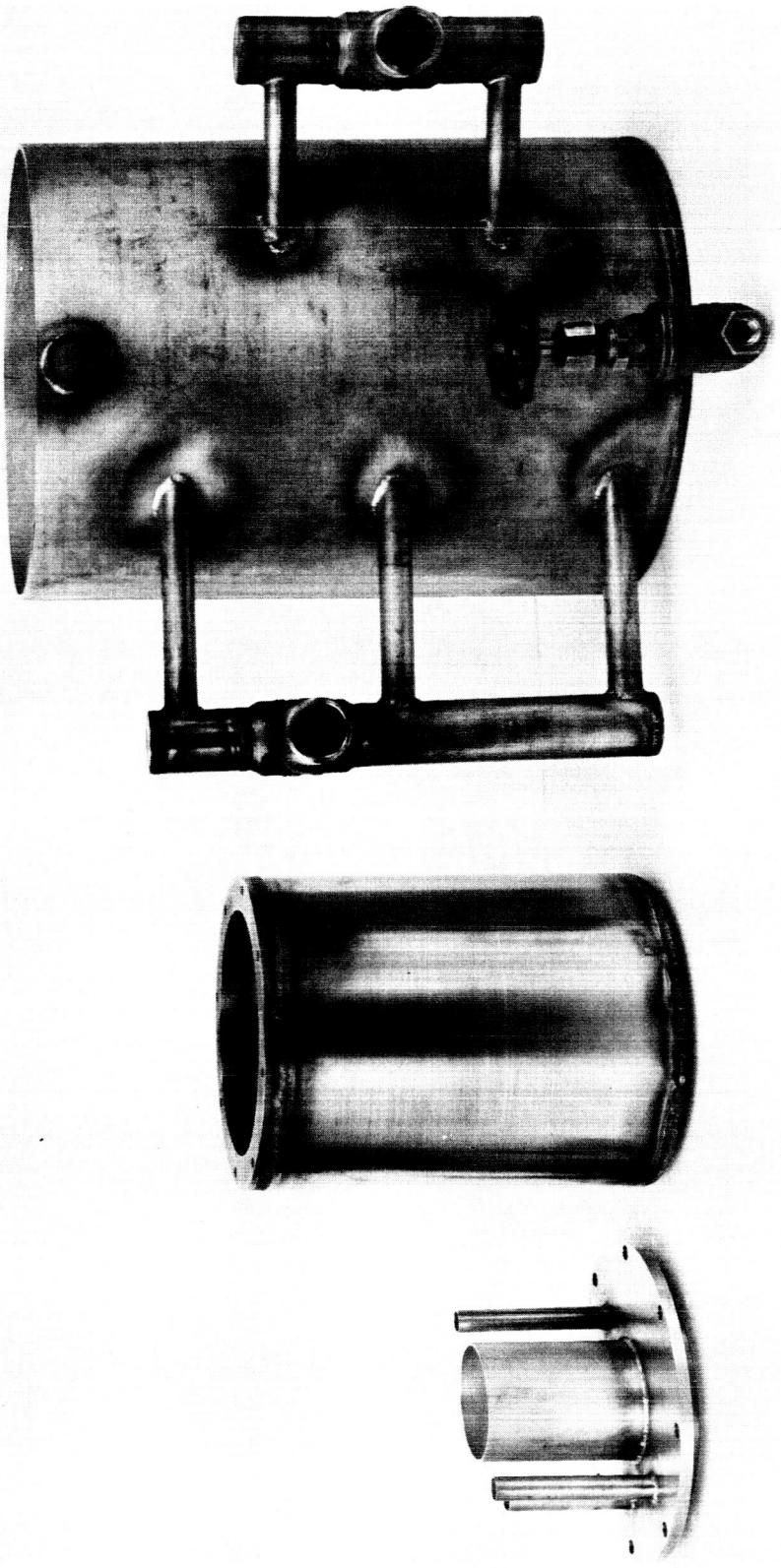

Figure 3. Calorimeter parts: cover, inner chamber, water jacket with intake and exhaust manifolds and drain valve.

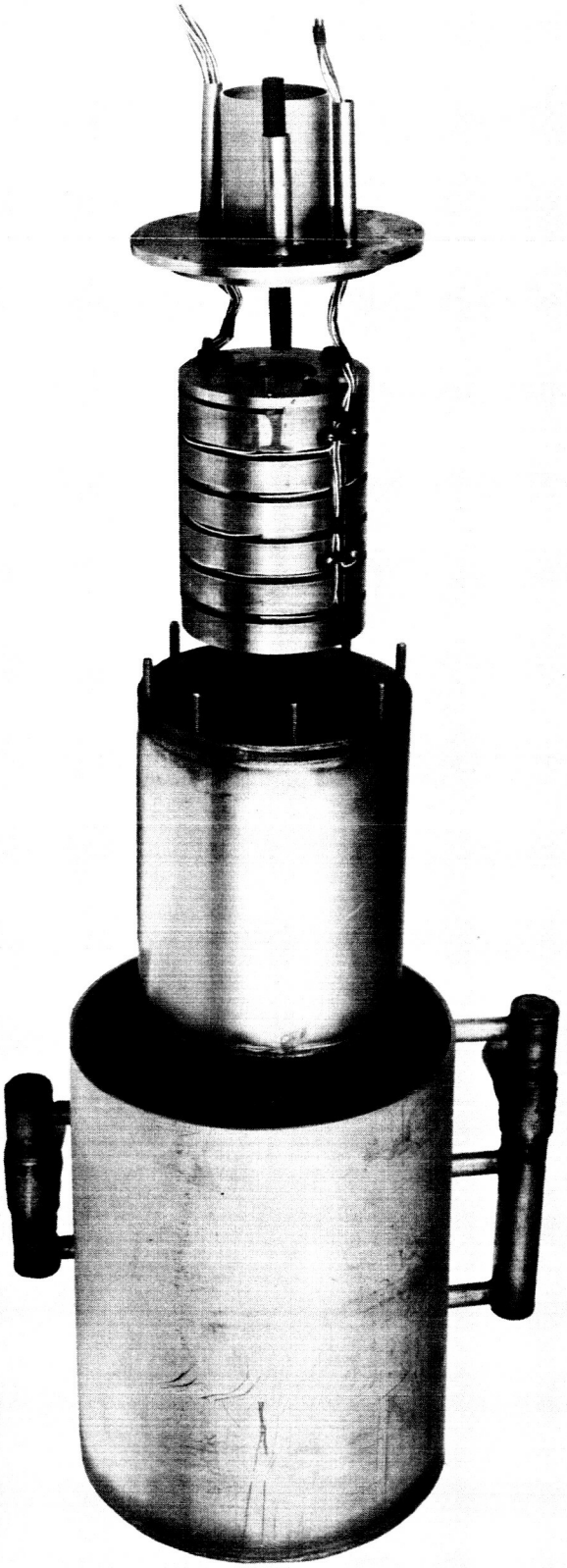

Copper Block

Inner Chamber

Water Jacket

Figure 4.

Exploded view of calorimeter assembly.

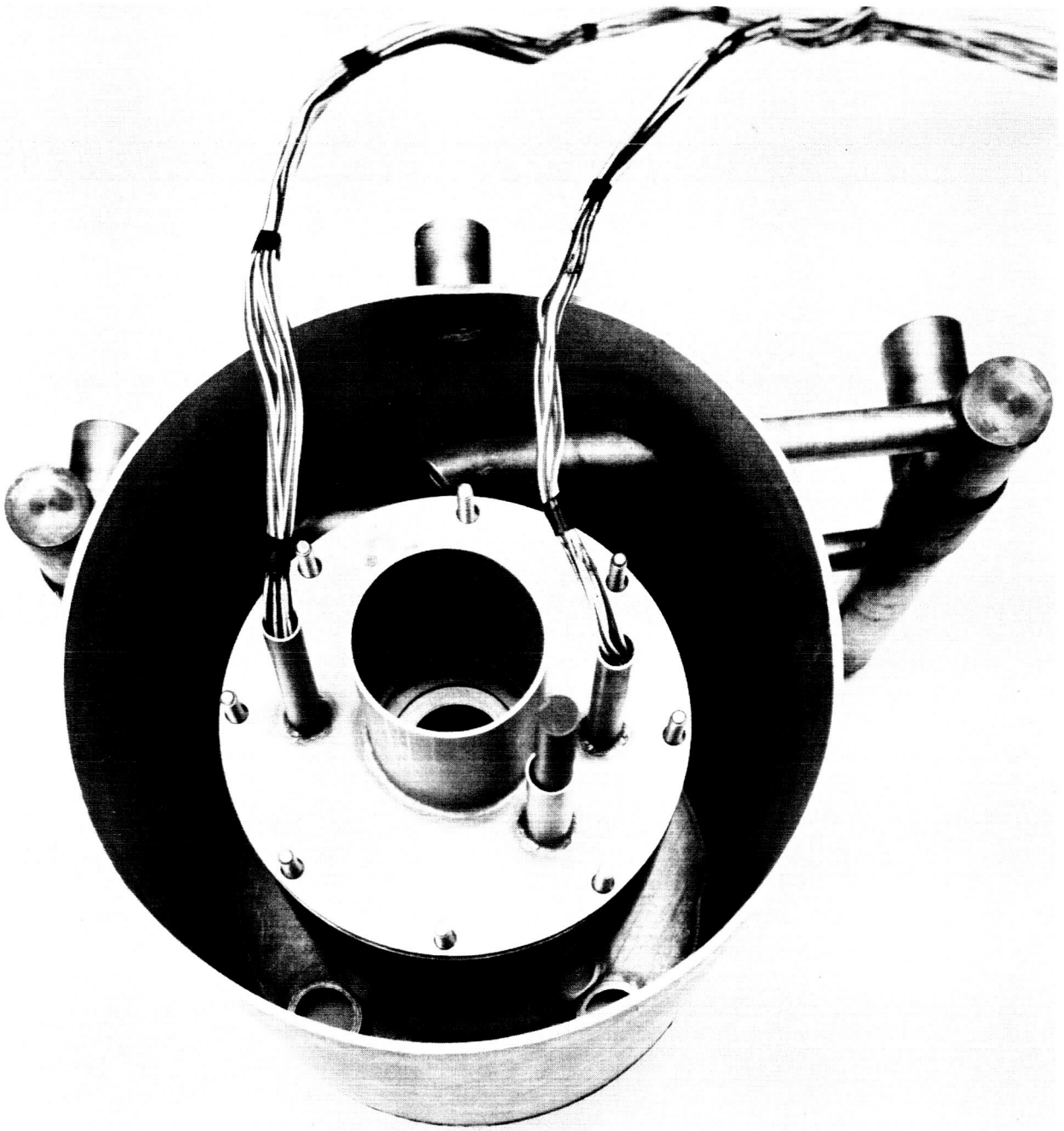

Figure 5. Assembled calorimeter. Holes in floor of water jacket are for electric heaters.

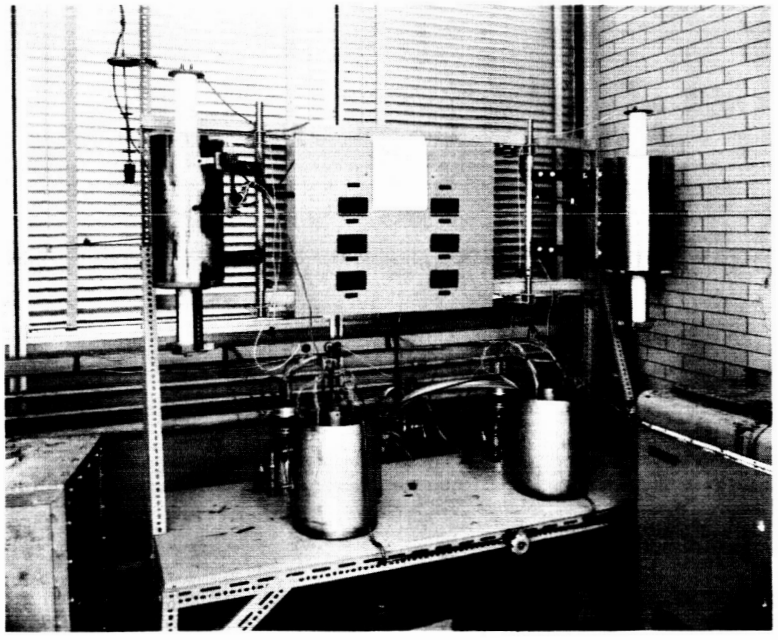

Figure 6. View of calorimeters and furnaces.

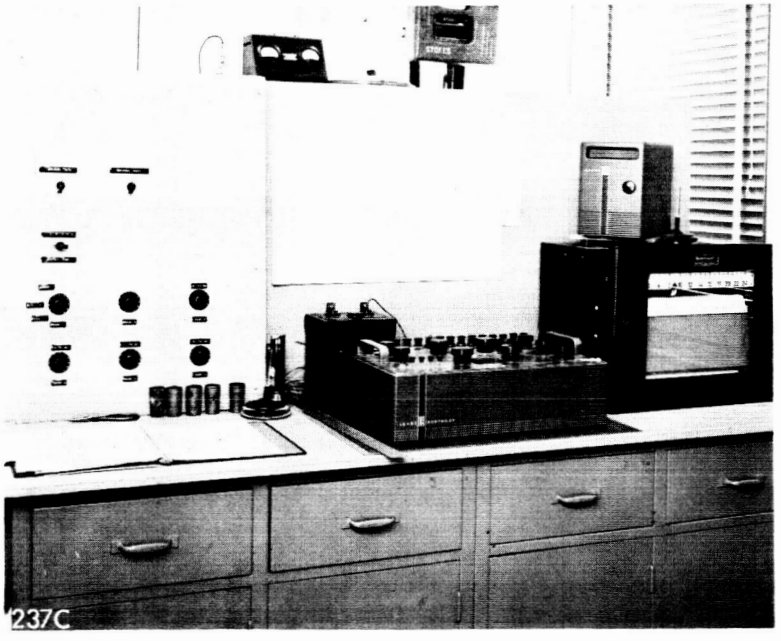

Figure 7. Measuring instruments and thermel switching panel.

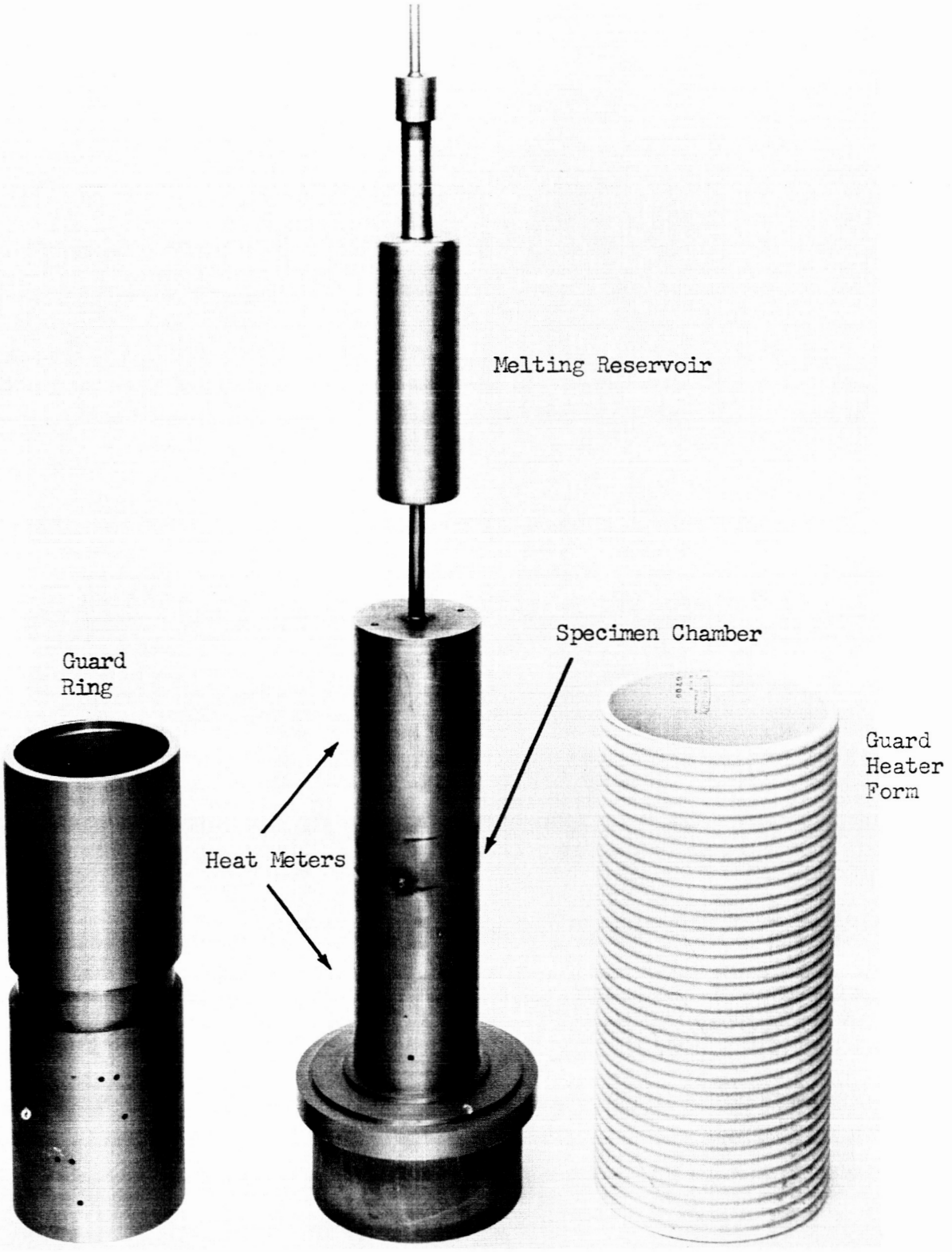

Figure 8. Guard ring, central specimen cylinder with melting reservoir, guard heater form.

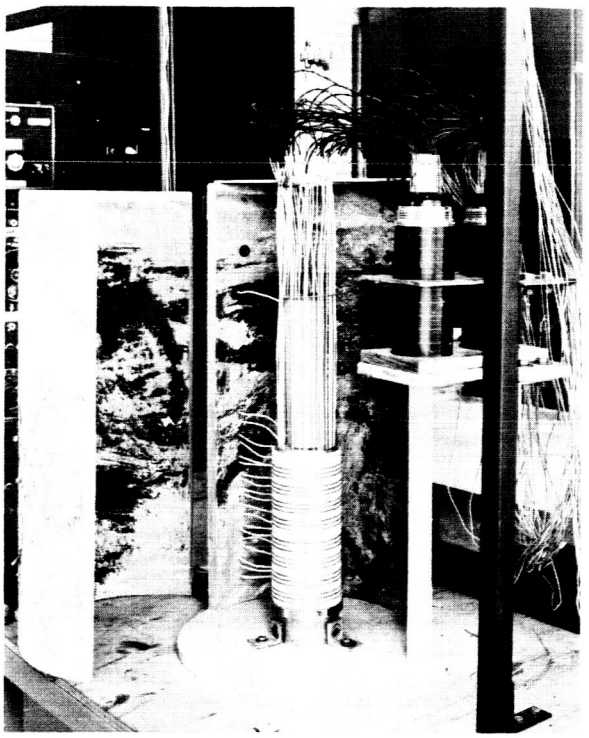

Figure 9. Thermal conductivity apparatus partly assembled.

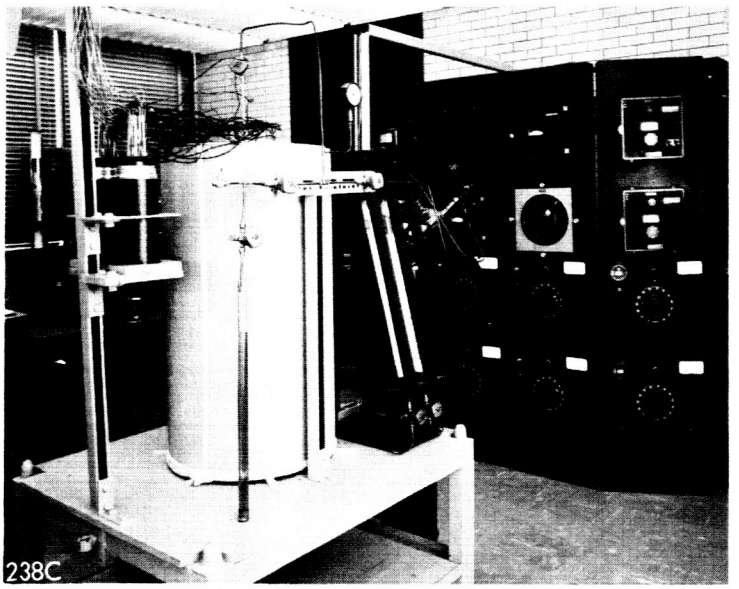

Figure 10. Thermal conductivity apparatus assembled. Hydrogen supply, purification system and bubbler are shown. Heater control panel is in background.

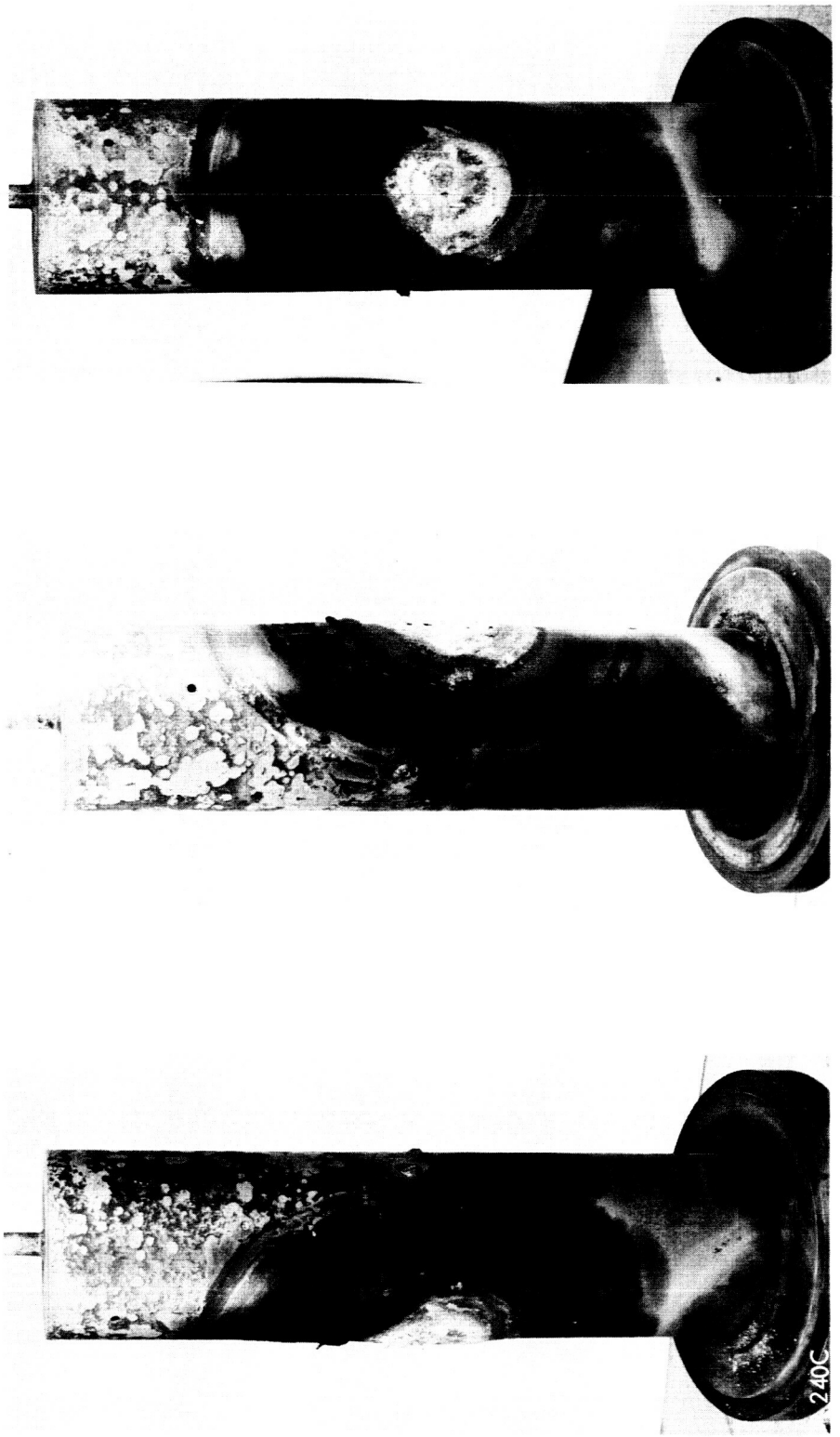

Figure 11. Views of thermal conductivity specimen cylinder after removal of guard ring.

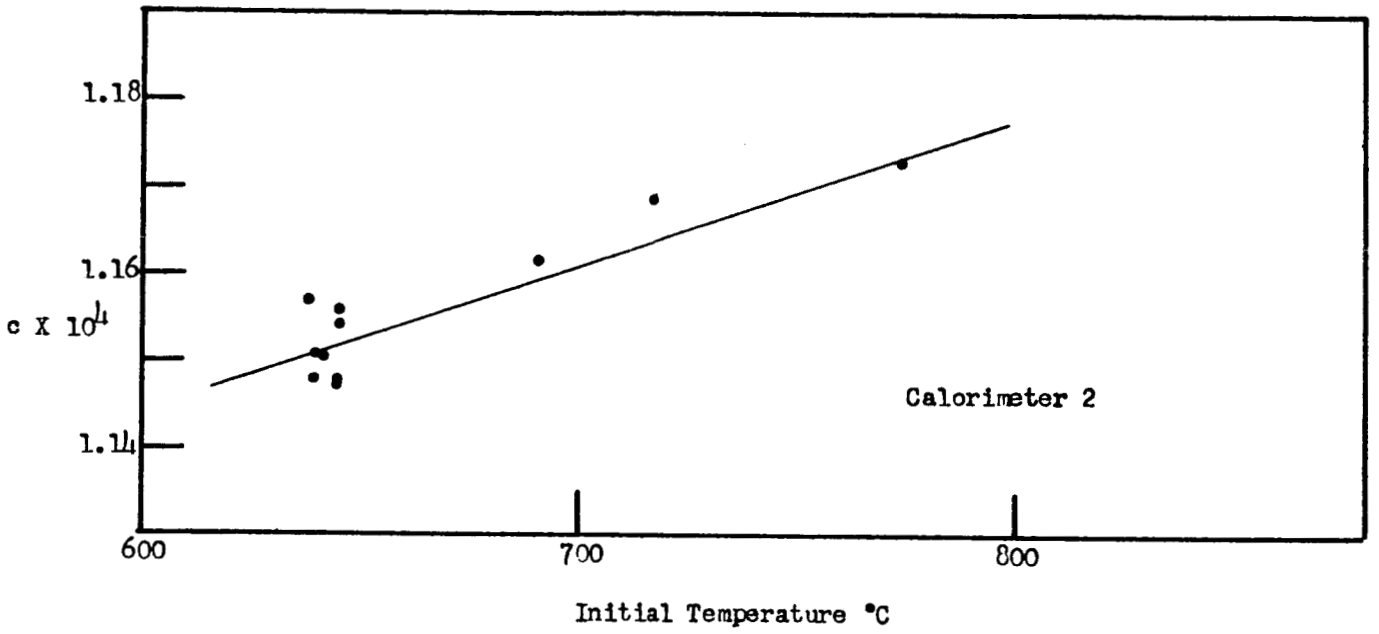

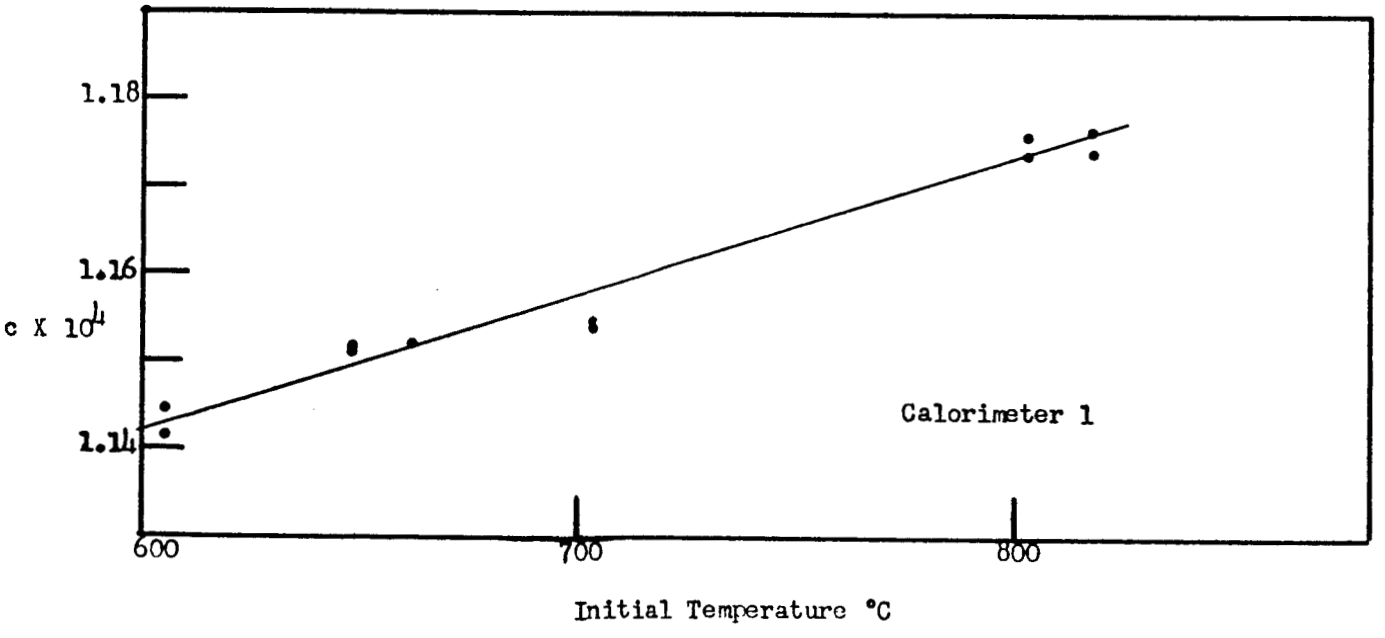

Fig. 12. Measured Values of c for the Empty Capsule.

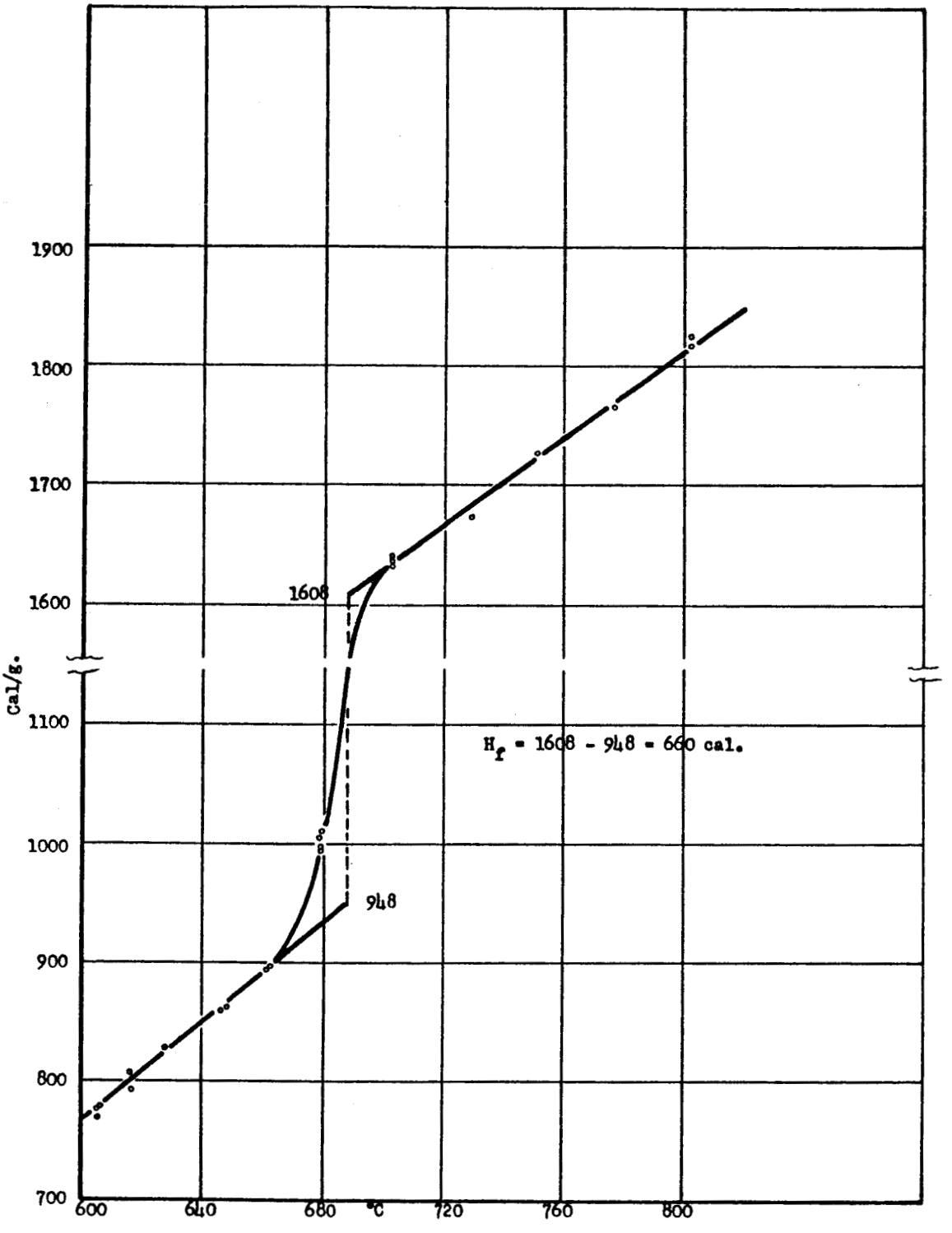

Figure 13. Enthalpy of Specimen I.

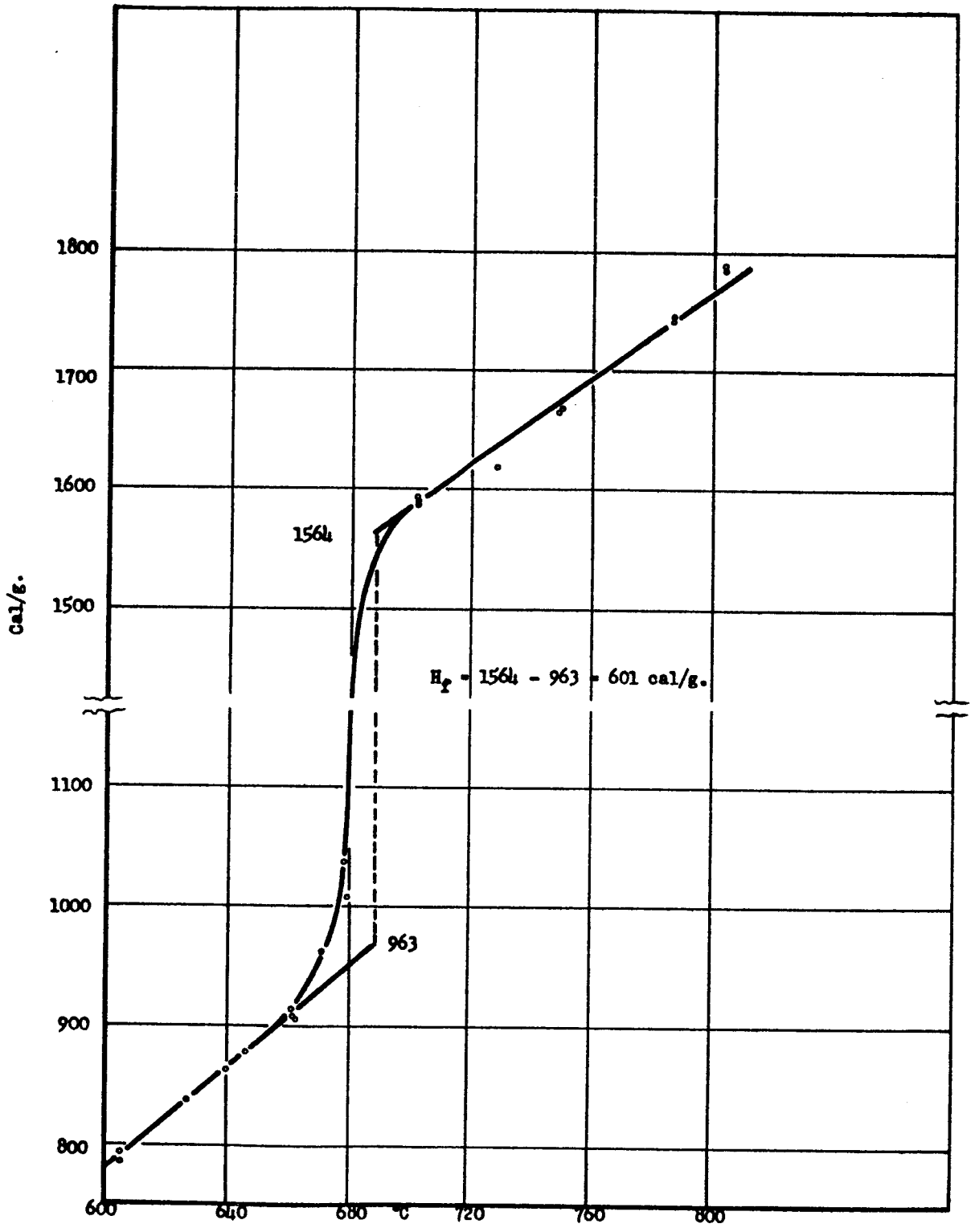

Figure 14. Enthalpy of Specimen J.

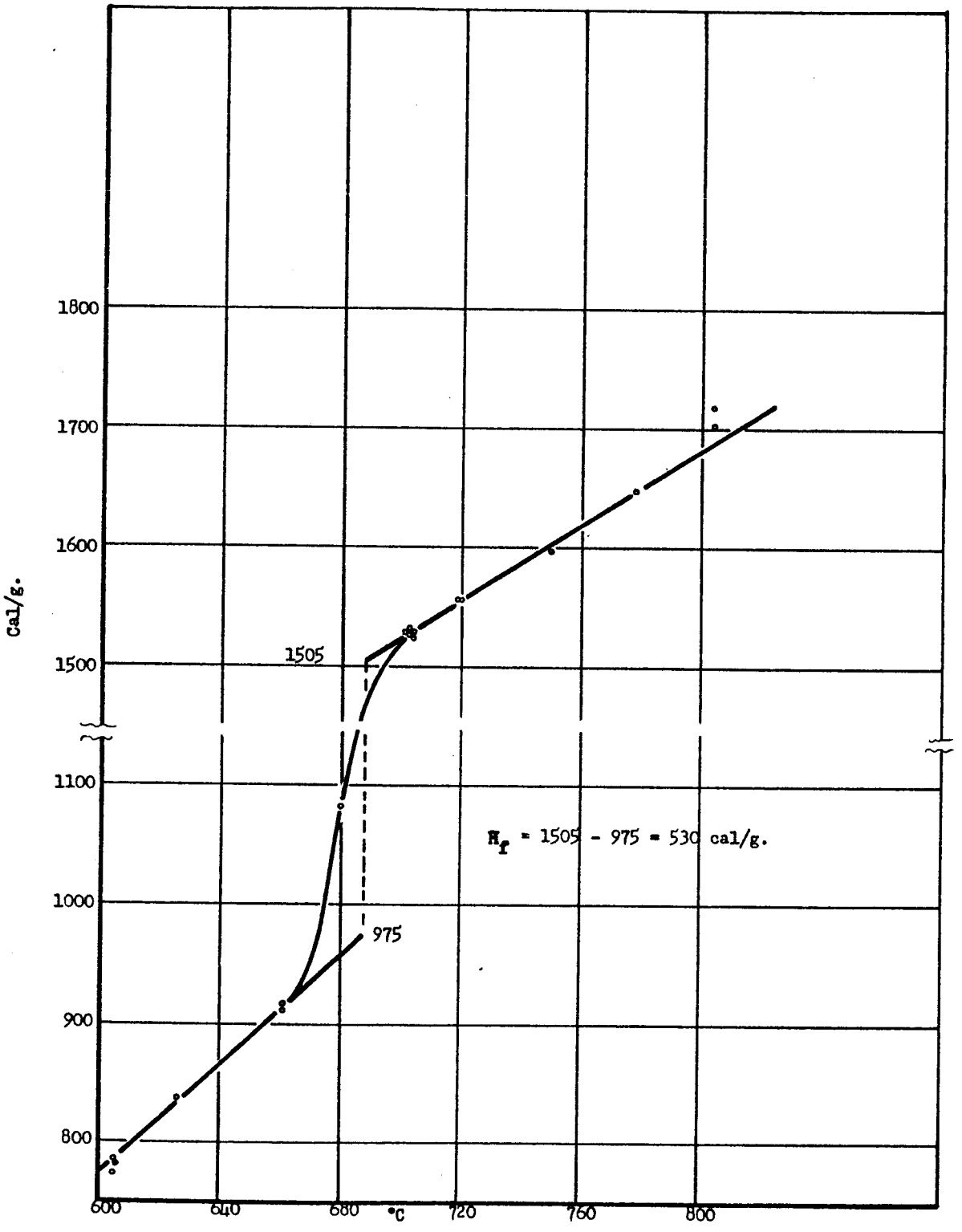

Figure 15. Enthalpy of Specimen K.

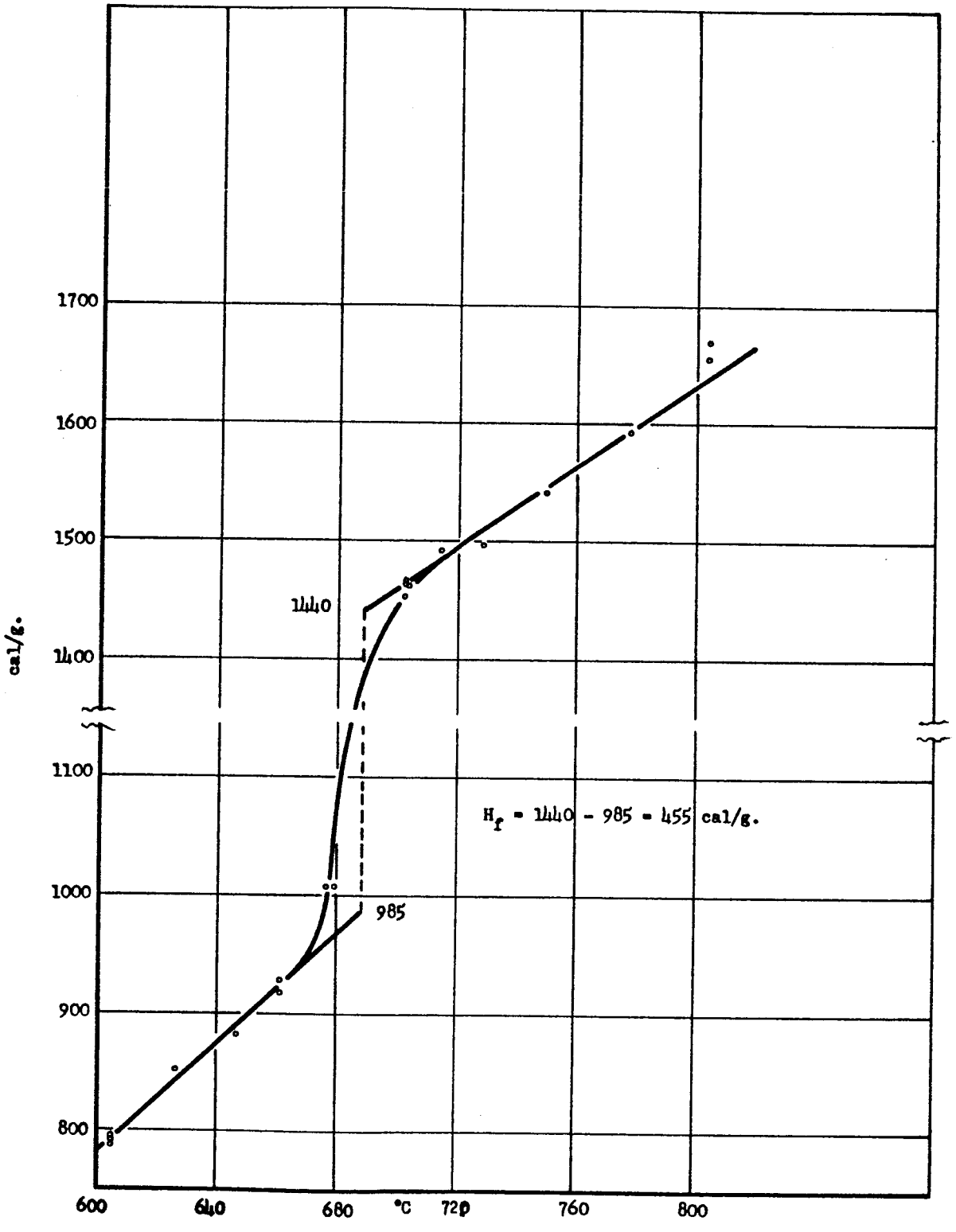

Figure 16. Enthalpy of Specimen L.

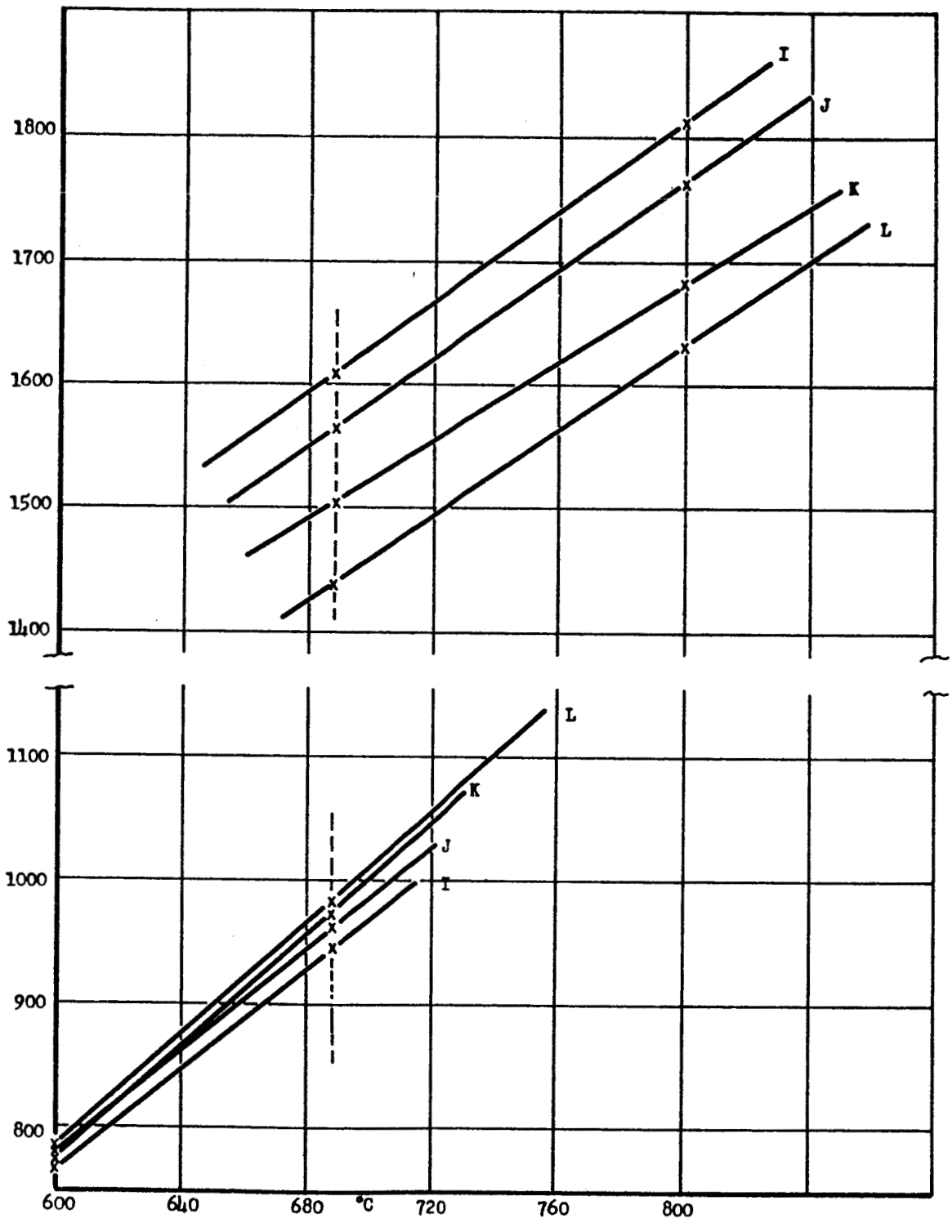

Figure 17. Smoothed Enthalpies of Specimens I, J, K, L.

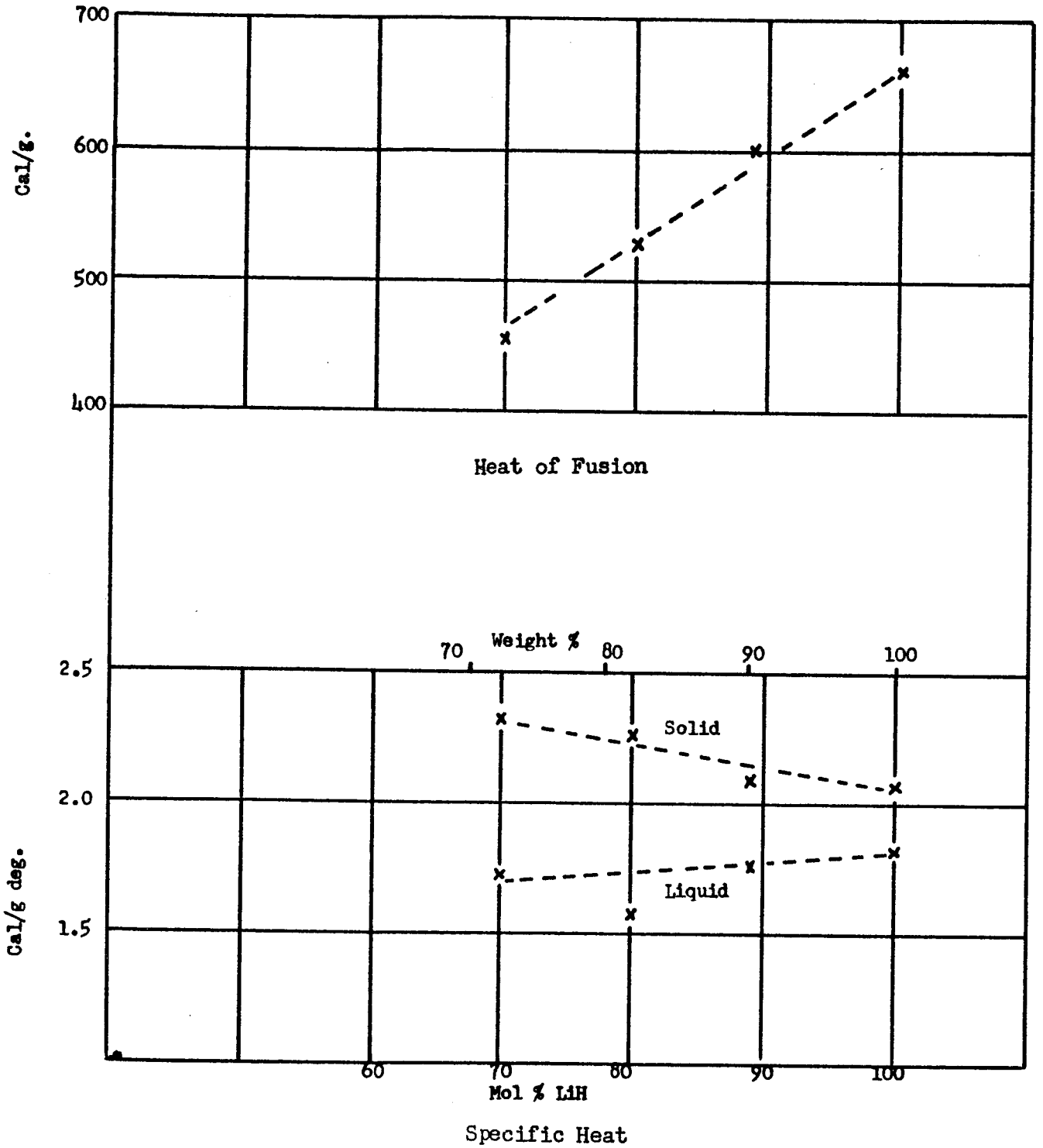

Figure 18. Heat of Fusion and Specific Heats as Function of Composition for Li-LiH Mixture.

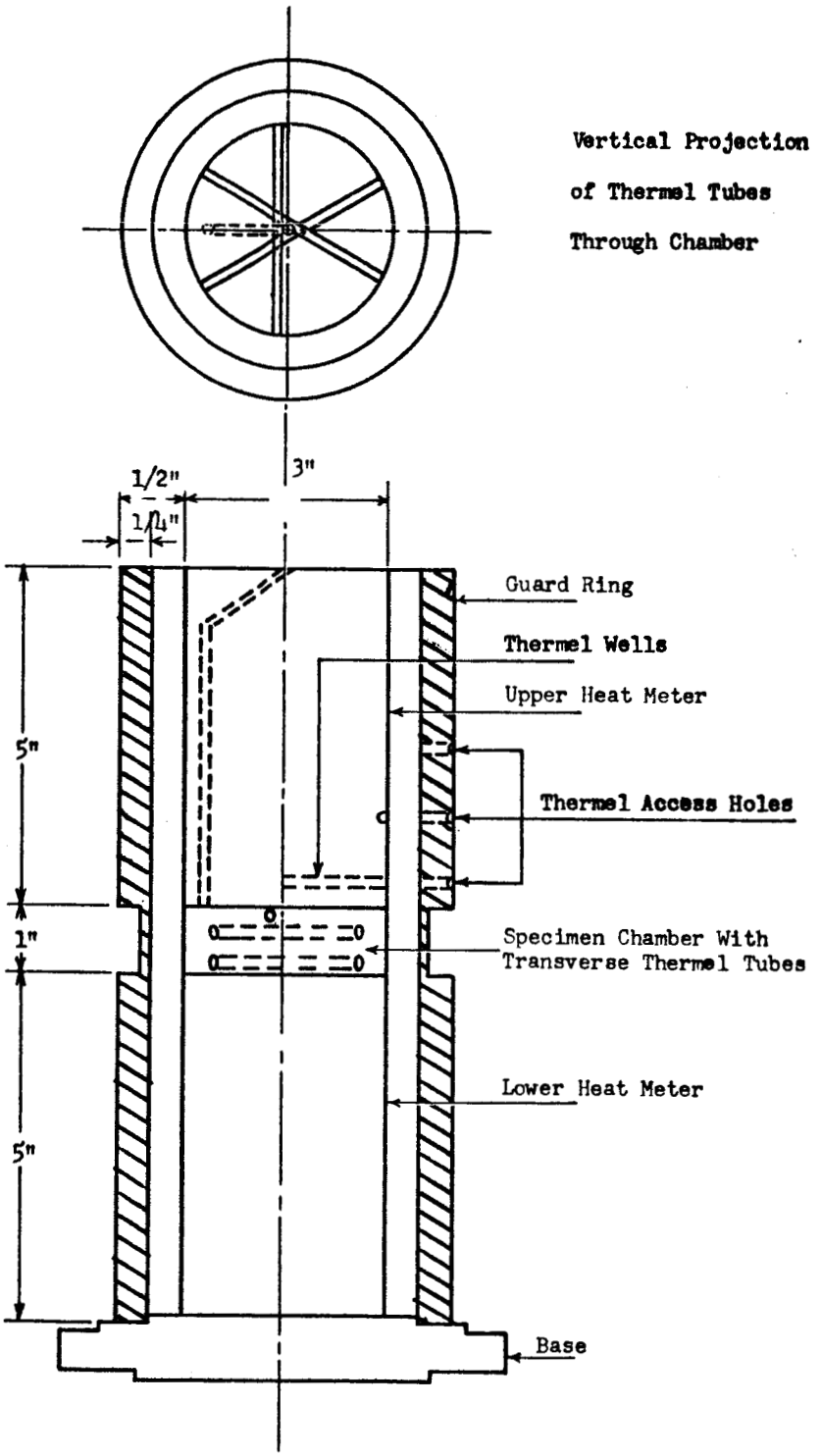

Figure 1. Vertical Section of Thermal Conductivity Apparatus

(Not drawn to Scale)

THERMAL CONDUCTIVITY TEST DATA

NO. 22

REMARKS: Powerstats set at (Midnight 26 May 61) (0001 hrs 27 May 61)

DATE 27 May 61

TIME 1420 hrs.

POWERSTAT READINGS

MAIN POWERSTAT: 100

(Reservoir heater)
10 50

(Specimen Top heater)
9 50

GUARD RING HEATERS
8. 34
7. 30
6. 45
5. 48 +4
4. 25
3. 30
2. 40
1. 40

Movable Thermocouple 34

1. 34.97	11. 34.97	21. 35.00	36. 32.67
2. 34.69	12. 34.605	22. 34.69	35. 37.82
3. 34.405	13. 34.445	23. 34.53	
4. 34.16	14. 34.09	24. 34.18	
5. 33.845	15. 33.74	25. 33.76	
31. 33.524			
32. 32.780			
33. 31.975			
6. 31.615	16. 31.955	26. 32.17	
7. 31.19	17. 31.39	27. 31.59	
8. 30.64	18. 30.94	28. 31.01	
9. 30.12	19. 30.31	29. 30.52	
10. 29.56	20. 29.74	30. 29.82	

Figure 20. Sample of Conductivity Data Sheet.

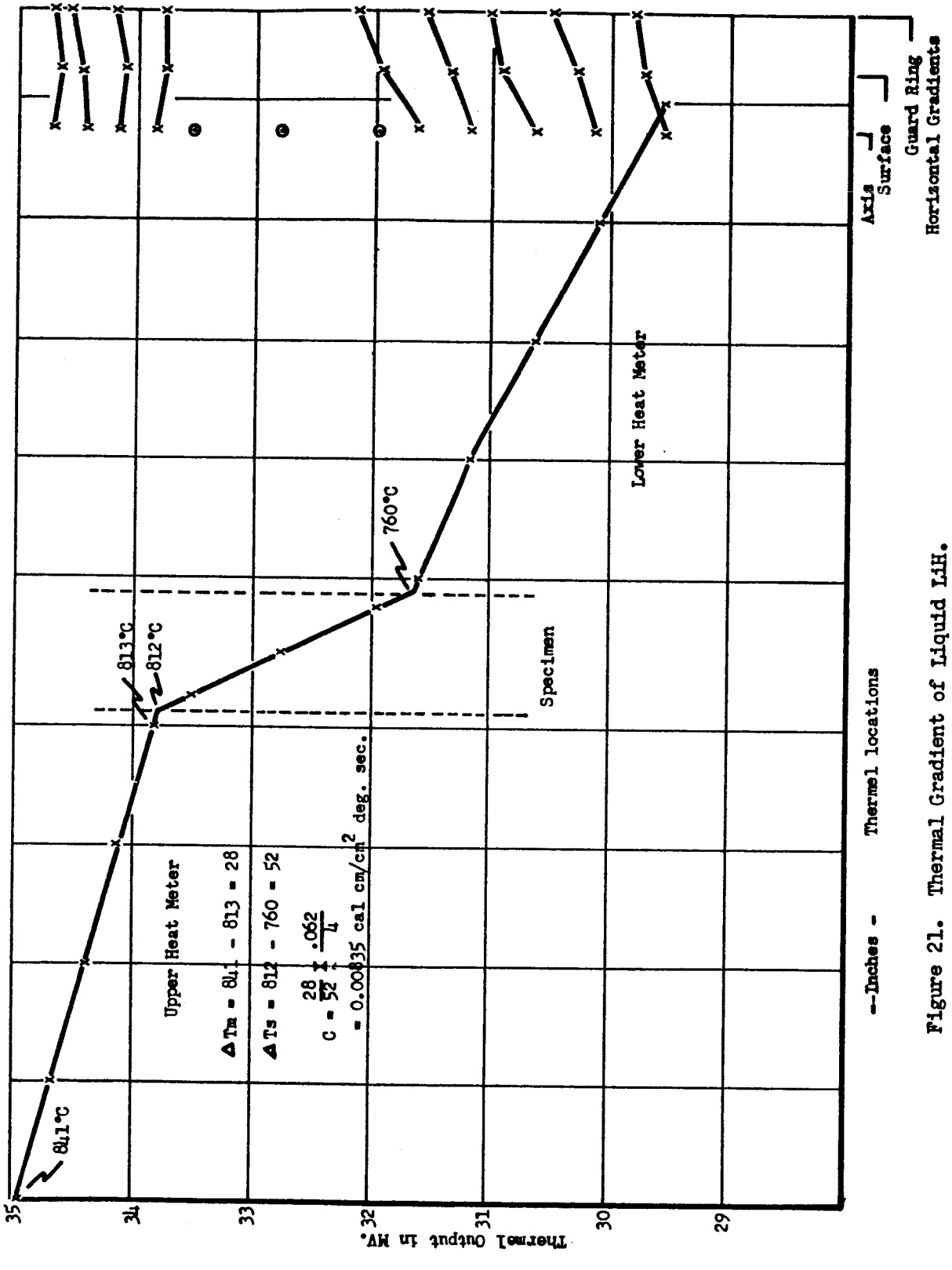

Figure 21. Thermal Gradient of Liquid LiH.

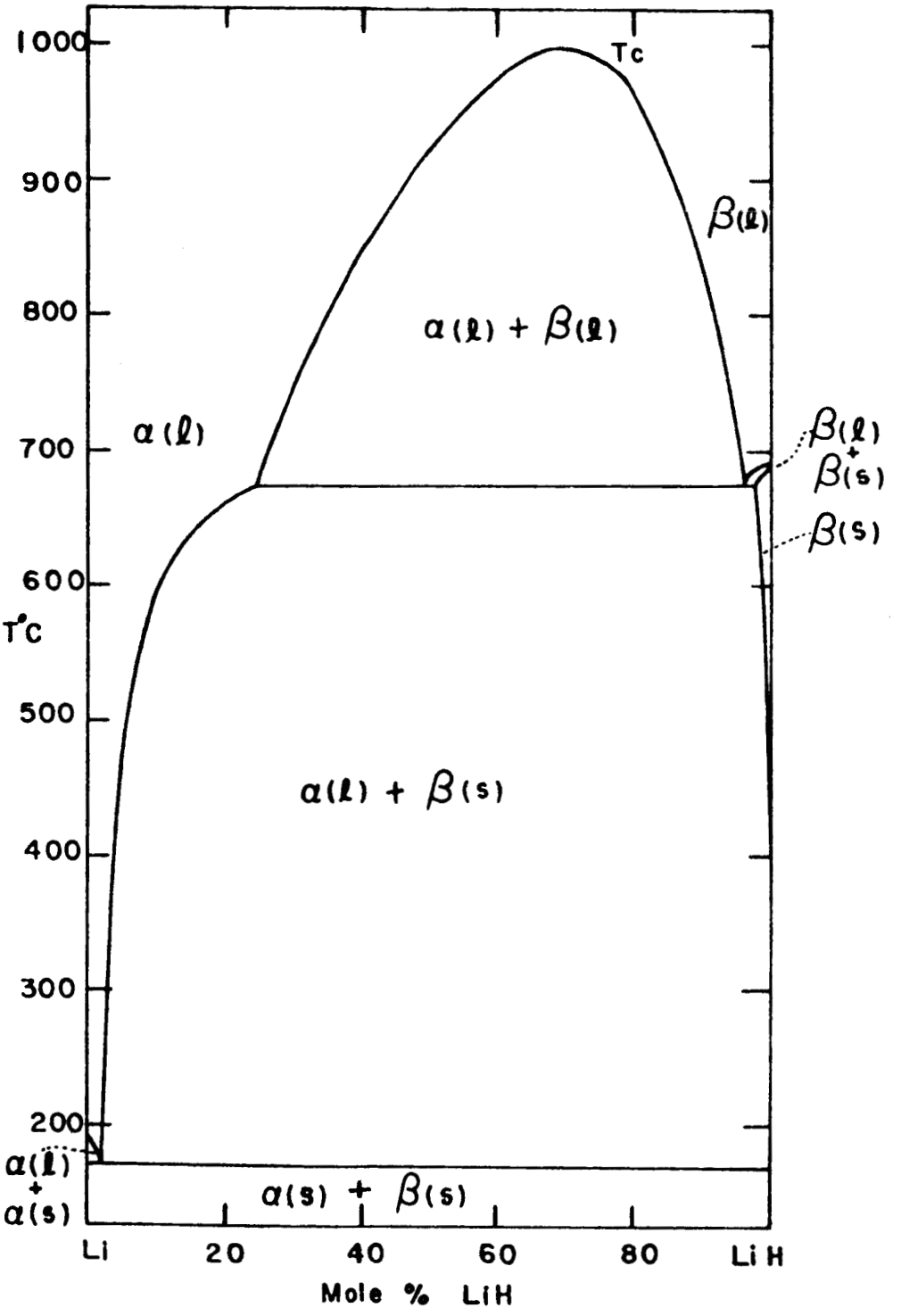

Figure 22. PHASE DIAGRAM (SCHEMATIC)
LITHIUM—LITHIUM HYDRIDE SYSTEM

From: A Survey Report on Lithium Hydride
C. E. Messer, October 1960 NYO-9470.

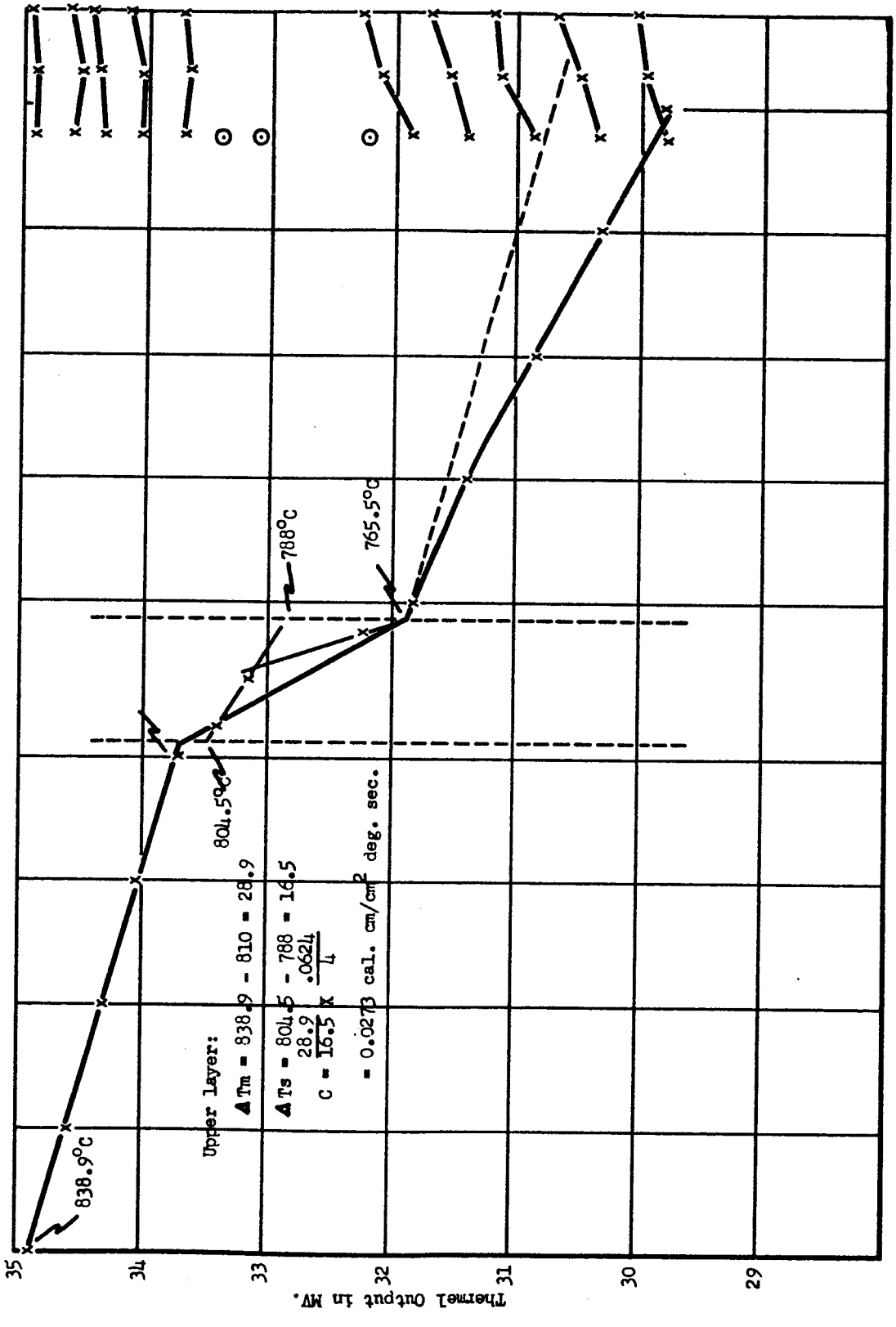

Figure 23. Thermal Gradient of Two-Phase Liquid System.

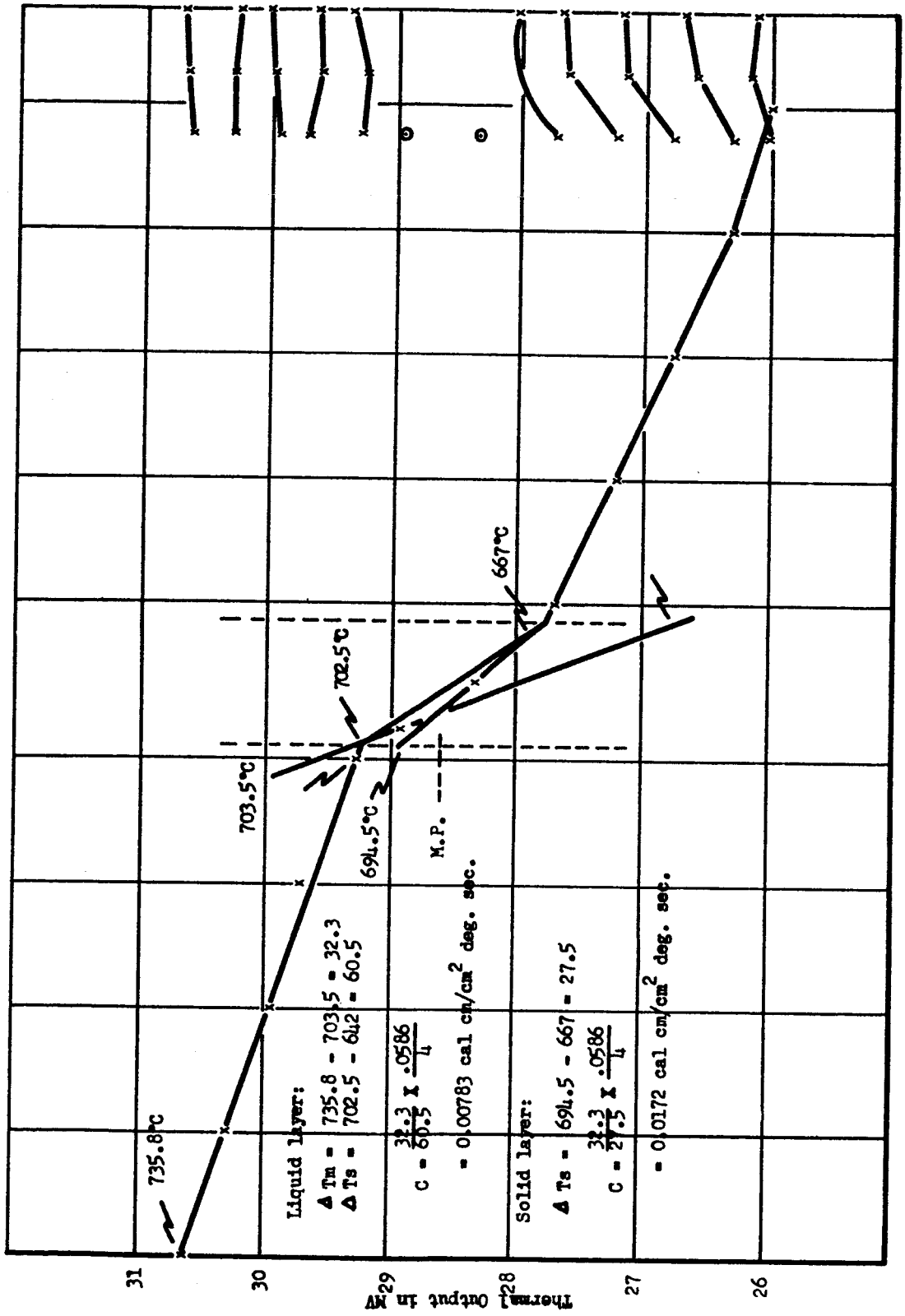

Figure 24. Thermal Gradient of Solid - Liquid.

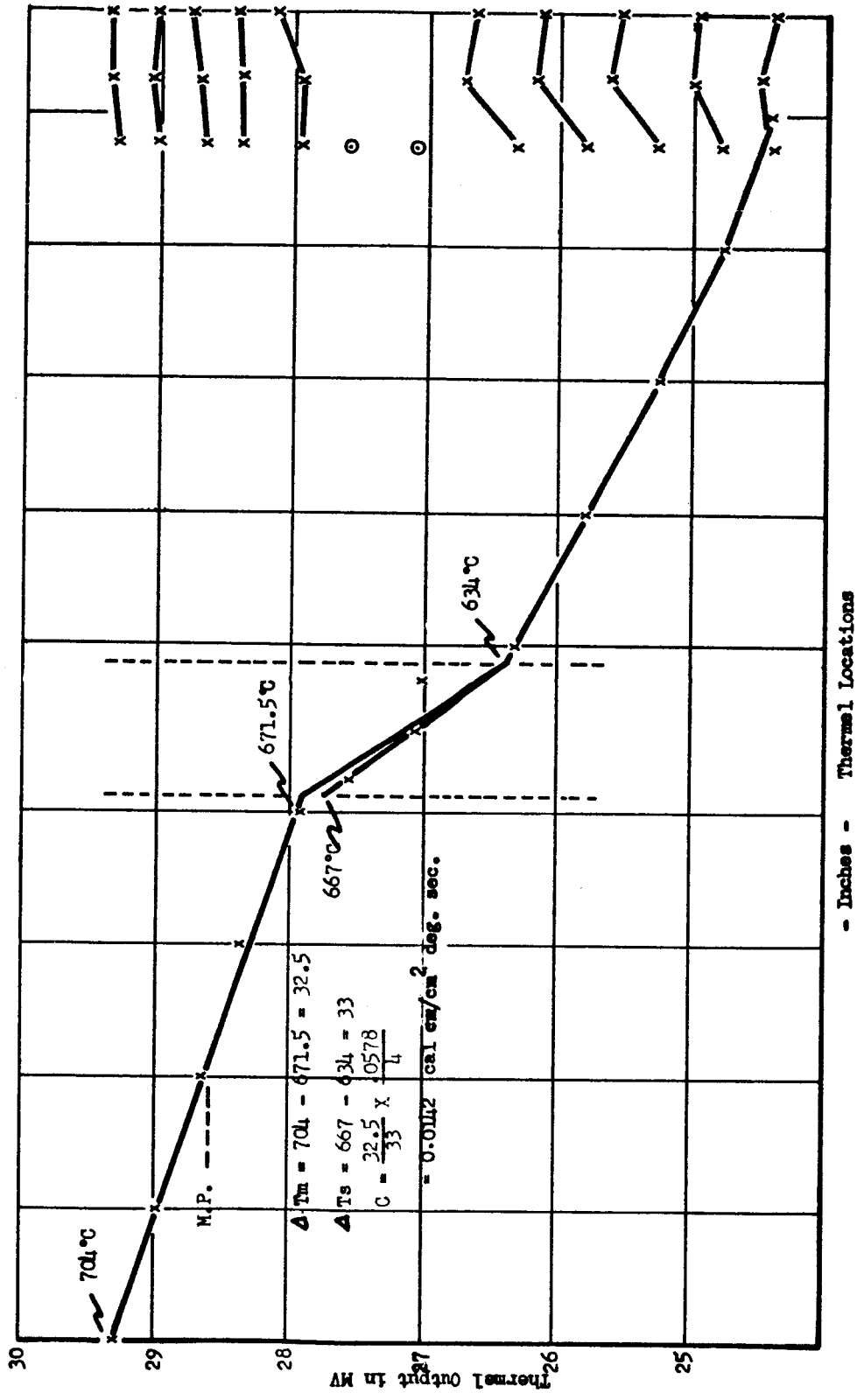

Figure 25. Thermal Gradient of Solid LiH.

APPENDIX II: TABLES

TABLE 1

ENTHALPY CHANGE OF SPECIMEN I (PURE LiH)
$(H_t - H_{30})$

t°C	cal/g mol	cal/g	Btu/lb.
605	6189	769	1383
605	6267	778	1401
605	6267	778	1401
616	6456	807	1453
626	6673	829	1492
627	6672	829	1492
646	6936	861	1550
648	6947	863	1553
661	7206	895	1611
661	7213	896	1613
679	7916	983	1770
679	8099	1005	1811
679	8142	1011	1820
680	8005	994	1789
702	13183	1637	2947
702	13136	1631	2937
702	13203	1640	2952
729	13470	1673	3011
751	13908	1728	3110
777	14223	1766	3180
802	14705	1826	3288
802	14637	1818	3272

TABLE 2

ENTHALPHY CHANGE OF SPECIMEN J

$(H_t - H_{30})$

t°C	cal/g mol	cal/g	Btu/lb.
605	6307	793	1427
605	6244	785	1412
627	6670	838	1507
640	6866	863	1554
646	6997	879	1583
661	7233	909	1636
661	7281	915	1647
661	7231	909	1636
671	7659	963	1733
678	8268	1039	1870
679	8024	1009	1815
702	12642	1589	2860
702	12629	1587	2857
702	12678	1593	2868
729	12878	1618	2913
750	13248	1665	2997
750	13255	1666	2999
787	13850	1741	3133
787	13879	1744	3140
804	14229	1788	3219
804	14197	1784	3212
804	14168	1781	3205

TABLE 3

ENTHALPY CHANGE OF SPECIMEN K

$(H_t - H_{30})$

$t\ ^{o}C$	cal/g mol	cal/g	Btu/lb.
605	6142	787	1416
605	6049	775	1395
605	6140	786	1415
626	6539	838	1605
661	7119	912	1641
661	7156	917	1650
680	8446	1082	1947
701	11944	1529	2754
702	11918	1526	2747
702	11920	1527	2748
702	11972	1533	2760
703	11939	1529	2752
703	11924	1527	2749
719	12146	1556	2800
719	12157	1557	2803
750	12496	1598	2876
778	12851	1648	2876
804	13433	1720	3097
804	13297	1703	3066

TABLE 4

ENTHALPY CHANGE OF SPECIMEN L

$(H_t - H_{30})$

t°C	cal/g mol	cal/g	Btu/lb.
605	6098	794	1429
605	6083	792	1425
605	6051	788	1418
626	6554	853	1535
646	6785	883	1590
661	7137	929	1672
661	7059	919	1654
676	7745	1008	1815
679	7752	1009	1816
702	11238	1464	2636
702	11261	1466	2639
702	11175	1454	2618
702	11256	1465	2637
714	11478	1494	2689
729	11483	1495	2690
750	11836	1541	2773
778	12249	1594	2870
804	12737	1658	2984
805	12833	1670	3006

TABLE 5A

ENTHALPY SUMMARY
c.g.s. UNITS
$H_t - H_{30} = A + Bt$
$\Delta H_f = H_{688(liquid)} - H_{688(solid)}$

Specimen	Mol %LiH	State	A	B	% Dev.	$H_{688}-H_{30}$ cal/g	ΔH_f cal/g
I	100	Solid	-484	2.087	0.4	951	
		Liquid	398	1.762	0.3	1610	659 ± 5
J	88.9	Solid	-400	1.977	0.45	960	
		Liquid	327	1.792	0.36	1560	600 ± 5
K	80.1	Solid	-639	2.352	0.3	979	
		Liquid	446	1.542	0.26	1507	528 ± 3
L	69.9	Solid	-518	2.173	0.7	977	
		Liquid	282	1.681	0.4	1438	461 ± 5

TABLE 5B

ENTHALPY SUMMARY
(ENGINEERING UNITS)
$H_t - H_{86} = A + Bt$
$\Delta H_f = H_{1270(liquid)} - H_{1270(solid)}$

Specimen	Mol %LiH	State	A	B	% Dev.	$H_{1270}-H_{86}$ Btu/lb.	ΔH_f Btu/lb.
I	100	Solid	-872	2.087	0.4	1712	
		Liquid	716	1.762	0.3	2900	1188 ± 9
J	88.9	Solid	-720	1.977	0.45	1729	
		Liquid	589	1.792	0.36	2808	1079 ± 9
K	80.1	Solid	-1151	2.352	0.3	1762	
		Liquid	803	1.542	0.26	2714	952 ± 3
L	69.9	Solid	-933	2.173	0.7	1760	
		Liquid	507	1.681	0.4	2590	830 ± 5

TABLE 6

CONDUCTIVITY OF MOLTEN LiH

Datum Number	Av. Specimen Temperature Deg. C	Conductivity Cal. cm/cm^2 Deg. C Sec.
18	792	.00827
20	778	.00825
21	778	.00857
22	786	.00835
27	703	.0090
32	713	.00881
34	715	.00828
55	711	.0112
56	717	.0104
57	717	.0102
59	728	.0100
60	738	.0099
63	760	.0104
65	772	.0094
69	777	.0084
85	712	.0111
86	728	.0111
87	725	.0106
89	710	.0107
105	718	.0106

TABLE 7

CONDUCTIVITY OF SOLID LiH AT THE MELTING POINT

Datum Number	Apparent Solid-liquid Interface Temp.	Cond. of Liquid Cal. cm/cm^2 Deg. C Sec.	Cond. of Liquid Cal. cm/cm^2 Deg. C Sec.
35	682°C	.013	--
41	630	.0172	--
42	629	.0173	--
43	687	.0167	--
47	687	.0168	--
48	687	.0170	.0080
49	687	.0167	.0078
50	687	.0167	.0085
52	687	.0180	.0078
53	695	.0179	.0079